UNIVERSITÀ POLITECNICA DELLE MARCHE

Faculty of Engineering

Master of Science Course in Biomedical Engineering

Parametric design of a mould for shaping custom made implants for orbital reconstruction

Supervisor: *Dr. Marco Mandolini*

Co-advisor: *Prof. Alida Mazzoli*

Master thesis of:

Elnaz Khorasani

Academic year:2019/2020

ABSTRACT

The aim of this study is to make parametric modelling of the implant for reconstruction of the bony orbital defect with restoration of anatomy, volume, function, and aesthetics. This innovative way describe workflow for 3D modelling and additive manufacturing (AM) of patient-specific medical implants which consist of medical imaging; 3D modelling; additive manufacturing; and clinical application. In the field of eyeball fractures, the most common orbital wall fractured was the floor, but combined wall fractures were frequent, and this method is suitable for modelling in each part of fracture in the cavity of eye bone. In other word, a patient-specific implant was digitally designed to reconstruct a facial bone defect. In the present study, an extensive post-traumatic orbital floor bone defect was reconstructed using a custom-made implant that was made with a selective laser melting (SLM) technique. In the last decade, an increasing number of dedicated software applications for surgical planning have been developed. Rapid prototyping (RP) technology refers to methods of fabrication that can create three dimensional (3D) objects from computer aided design (CAD) datasets, sometimes simply known as 3D printing and the development of new fabrication methods has resulted in rapid prototyping technology becoming highly accessible, cost-effective and fast . Design methods for the reconstruction of cranio-maxillofacial defects include the use of a pre-operative model printed with pre-operative data, printing a cutting guide or template after virtual surgery, a model after virtual surgery printed with reconstructed data using a mirror image, and manufacturing patient-specific implants (PSIs) by directly obtaining PSI data after reconstruction using a mirror image. Different Materials such as titanium, polyethylene, polyetheretherketone (PEEK), hydroxyapatite (HA), poly-DL-lactic acid (PDLLA), polylactide-co-glycolide acid (PLGA), and calcium phosphate are used. By selecting the appropriate design method, manufacturing process, and implant material according to the case, it is possible to obtain a more accurate surgical procedure, reduced operation time, the prevention of various complications that can occur using the traditional method, and predictive results compared to the traditional method . Reverse Engineering (RE) process consented the reconstruction of the craniofacial defect starting from CT scans converted thus into a 3D mathematical model. Rhinoceros V.6.28 modelling software allowed for the parametric modelling of implant and related mould that totally fit the designed

implant. Thus, after modelling the defect part of orbit with plugin of Grasshopper of Rhinoceros software export .stl format file for creating the computer-designed implant that has the proper geometry and fit perfectly into the defect without requiring any intraoperative adjustments. As total, thanks to this anatomical approach in which the methodology results to be reproducible to any other orbital wall defect and different patients.

Future research should consider the potential effects of algorithm modelling in Grasshopper in the field of medicine more carefully, for example defining plugin in Grasshopper which will be able to modelling of the orbital with more precision in minim of time.

KEYWORDS

orbital wall reconstruction, Reverse engineering, Computer aided design, Custom Implants, Additive manufacturing (AM),3D printing, imaging data, maxillofacial surgery, Biomedical design.

Abstract

Lo scopo di questo studio è quello di realizzare la modellazione parametrica dell'impianto per la ricostruzione del difetto osseo orbitale con ripristino di anatomia, volume, funzione ed estetica. Questo modo innovativo descrive il flusso di lavoro per la modellazione 3D e la produzione additiva (AM) di impianti medici specifici per il paziente che consistono in imaging medico; Modellazione 3D; produzione di additivi; e applicazione clinica. Nel campo delle fratture del bulbo oculare, la frattura della parete orbitale più comune era il pavimento, ma le fratture della parete combinate erano frequenti e questo metodo è adatto per modellare ogni parte della frattura nella cavità dell'osso dell'occhio. In altre parole, un impianto specifico per il paziente è stato progettato digitalmente per ricostruire un difetto osseo facciale.

LIST OF FIGURES

List of tables:

TABLE OF CONTENTS

INTRODUCTION

Orbital wall fractures can result in increased orbital volume [1] and in approximately 8.5% of patients, increased orbital volume remains after treatment with traditional reconstruction techniques [2,3].

Orbital fractures are frequently observed in maxillofacial traumas and can produce a wide range of functional disabilities and aesthetic deformities [4,5]. fractures of the internal orbit can cause several problems, including ocular muscle entrapment limiting extrinsic eye movements, diplopia, enophthalmos, vertical displacements of the globe, sinusitis, and loss in visual acuity. fractures frequently reported are mainly associated with high-energy trauma, motor vehicle collisions, violent assault and many other causes such as tire explosions, ruptured garage door springs, chainsaws, high-voltage electric shocks, swinging objects, falls from high places, and objects that crush and etc [6,7].The manual process for preparing implant is very labour intensive and expensive. Alternatively, it is possible to create custom made patient specific implants by using 3D modelling software and additive manufacturing (AM). This process has potential for more accurate and cost-effective implants. Preoperative models are commonly used for planning or simulating difficult sections of surgical operations. It is possible to design patient-specific implants digitally by using computed tomography (CT) images as a reference and by manufacturing the implant with traditional machining methods [8,9]. We aimed at developing a workflow for 3D modelling and AM of patient-specific medical implants. Traditional techniques for maxillofacial implants fabrication rely on the skills of the surgeon in manually carving a wax cast to accurately match the patient's anatomy, requiring thus a long time of development [10,11]. Different approaches based on anatomical or mathematical features of the eyeball surface are available for the reconstruction of an orbital defect according to their size and shape: mirror-imaging of the unaffected side [12], thin plate spline surface interpolation [13] and anatomical reconstruction [14]. the present study defines the procedure for the creation of an implant for orbital floor intended to a young boy.

A briefly overview of eyeball bones in a way to better understand and justify the choices that contribute to the definition of an adequate procedure to design the implant. Moreover, a section of the thesis is devoted to the presentation of the historical evolution of prosthetic implants and related materials. Besides this, a review of the current techniques adopted in orbital

cavity reconstruction field has been updated with the rapid prototyping technologies utilized in the fabrication of a solid 3D implant.

Basically, the first step for starting the process of designing and production of the implant is acquired the Computed tomography (CT) Scan images (Input) at first in the Mimics software and then in Rhinoceros software (Grasshopper plugin). Materialise's Interactive Medical Image Control System (MIMICS) is an interactive tool for the processing and the visualization of CT images as well as MRI images and 3D rendering of objects. Briefly the volume and 3 dimensional shape of healthy orbit of eye acquired and then mirrored the healthy part of eye to the pathological side .As geometric variability between the two orbital cavities is possible because the human face is not symmetric, particularly in people with cranial trauma For this reason and to ensure the restoration of orbital volume and aesthetics of the pathological side, it needs to be operated before on the mirrored healthy orbital cavity and then on the pathological one[15].

The result was obtained by 3D printing fabrication of a mould characterized by a punch and a matrix involved in a pressure mechanism able to shape a layer of Medpor material embedded with a Titanium mesh, according to the previously designed implant. The need for the last-mentioned material justified the choice of this second proposed procedure that differs only in the last step of the design, by showing evidence of the importance of CAD additive manufacturing technologies in maxillofacial reconstruction field.

1.anatomy of orbit

In anatomy, the orbit is the cavity or socket of the skull in which the eye and its appendages are situated. "Orbit" can refer to the bony socket. In the adult human, the volume of the orbit is 30 millilitres of which the eye occupies 6.5 ml [16]. The bony walls of the orbital canal in humans do not derive from a single bone, but a mosaic of seven embryologically distinct structures (Figure 1) [17]. Bone is the main supporting tissue of the body in terms of load bearing, despite it is a very lightweight material. Its composition includes protein (collagen about 90% to give flexibility) and mineral (crystals of hydroxyapatite

impregnate the collagen matrix to make the structure more stiff) that can repair and reshape itself in response to external stresses[18].

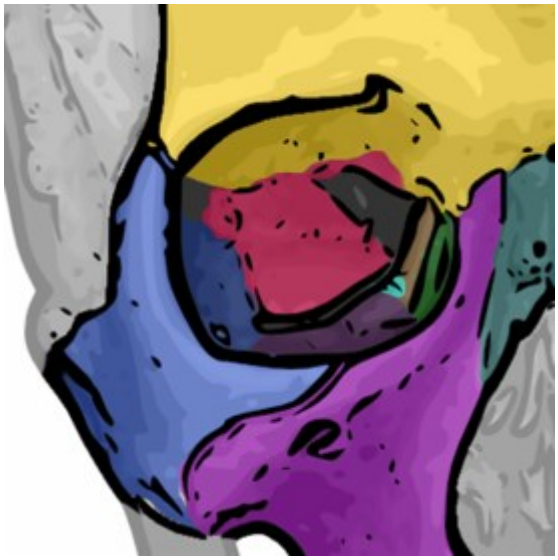

Figure 1: The seven bones that form the orbit: yellow = Frontal bone, green = Lacrimal bone brown = Ethmoid bone, blue = Zygomatic bone, purple = Maxillary bone, aqua = Palatine bone, red = Sphenoid bone

1.1 Borders and Anatomical Relations

The orbit is a bony pyramid with four walls: a roof, lateral wall, floor, and medial wall. The base of the pyramid is the orbital entrance, which is roughly rectangular the boundaries of the orbit are formed by seven bones. It is also important to consider the anatomical relations of the orbital cavity – this is clinically relevant in the spread of infection, and in cases of trauma [19].

The borders and anatomical relations of the bony orbit are as follows (Figure 2):

- ***Roof** (superior wall) – Formed by the frontal bone and the lesser wing of the sphenoid. The frontal bone separates the orbit from the anterior cranial fossa.*
- ***Floor** (inferior wall) – Formed by the maxilla, palatine, and zygomatic bones. The maxilla separates the orbit from the underlying maxillary sinus.*
- ***Medial wall** – Formed by the ethmoid, maxilla, lacrimal and sphenoid bones. The ethmoid bone separates the orbit from the ethmoid sinus.*
- ***Lateral wall** – Formed by the zygomatic bone and greater wing of the sphenoid.*
- ***Apex** – Located at the opening to the optic canal, the optic foramen.*

- ***Base*** *– Opens out into the face and is bounded by the eyelids. It is also known as the orbital rim.*

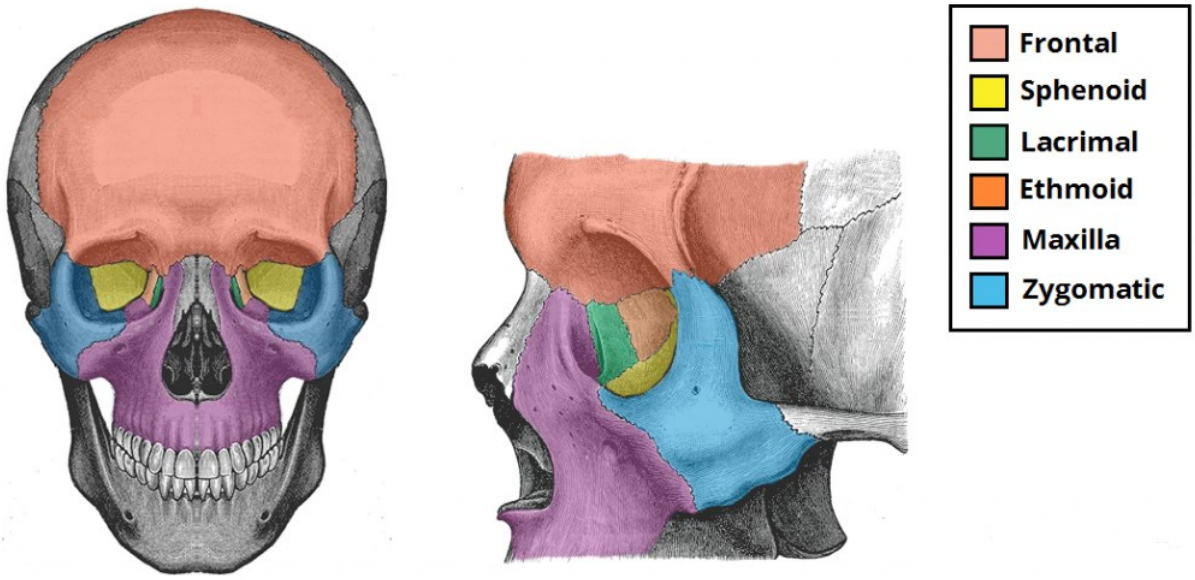

Figure 2: The borders of the bony orbit

1.2. Pathways into the Orbit

There are three main pathways by which structures can enter and leave the orbit (Figure 3):

- *Optic canal – transmits the optic nerve and ophthalmic artery.*
- *Superior orbital fissure – transmits the lacrimal, frontal, trochlear (CN IV), oculomotor (CN III), nasociliary and abducens (CN VI) nerves. It also carries the superior ophthalmic vein.*
- *Inferior orbital fissure – transmits the zygomatic branch of the maxillary nerve, the inferior ophthalmic vein, and sympathetic nerves [19].*

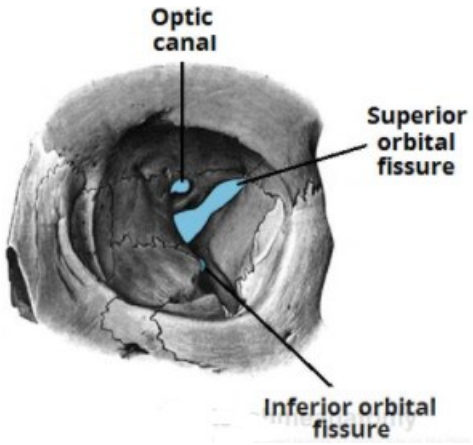

Figure 3: Pathways into the Orbit

The medial orbital walls are parallel, approximately 2.5 cm apart and separated by paired ethmoid sinuses [20]. Each lateral wall forms a 45^{o} angle with its respective medial wall, resulting in 90^{o} between the two lateral walls (Figure 4).

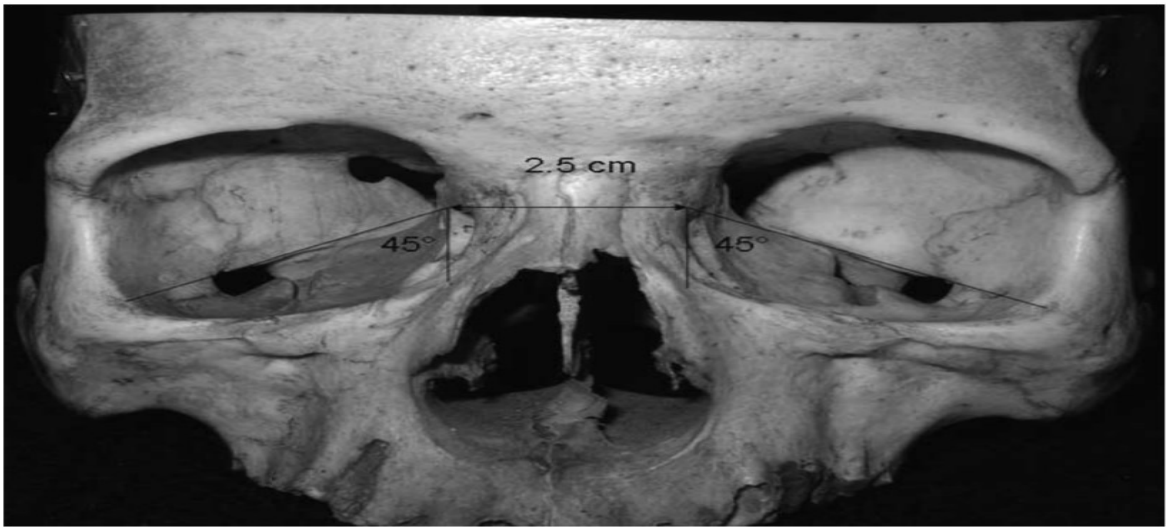

Figure 4: The relationship between the medial walls, the paired ethmoid sinuses, and the corresponding lateral walls

2. Eye Socket Fracture (Fracture of The Orbit)

The eye socket is a bony cup that surrounds and protects the eye. The rim of the socket is made of thick bones, while the floor and nasal side of the socket is paper thin in many places. A fracture is a broken bone in the eye socket involving the rim, the floor or both.

I. Orbital rim fracture

This injury affects the bony outer edges of the eye socket. Car accidents are one of the main causes of this kind of fracture.

II. Blowout fracture

A blowout fracture is an isolated fracture of the orbital walls without compromise of the orbital rims [24]. fracture is a break in the floor or inner wall of the orbit of eye socket. Getting hit with a baseball or a fist often causes a blowout fracture. The theories of the pathophysiological mechanisms of occurrence of these fractures could be called hydraulic theory. It says that the force is transmitted through the impact on the eyeball, which suffers retro propulsion raising the intra-orbital. This pressure is transmitted to or less than the medial wall, while orbital rim remains intact. The second theory is explained by the direct impact of force on the orbital rim, with the force being transmitted to the lower wall thickness, causing the fracture (Figure 5) The treatment of blow-out fractures is a major challenge for the Maxillofacial Surgeon and selection of the biomaterial is related to several factors, such as the size of the defect, the number of walls involved the adaptation of internal contours, restoration of appropriate volume, elapsed time of the trauma and the experience of the surgeon [23].

III. Orbital floor fracture

This is when a blow or trauma to the orbital rim pushes the bones back, causing the bones of the eye socket floor buckle to downward. This fracture can also affect the muscles and nerves around the eye, keeping it from moving properly and feeling normal [21]. Orbital fractures are more common in males than in females and most often occur in men, ages 21 to 30 years of age [25]. Fractures of the orbital floor and the medial orbital wall are the most common fractured site [26]. Falls, motor vehicle accidents, and assaults account for most midfacial fractures [27].

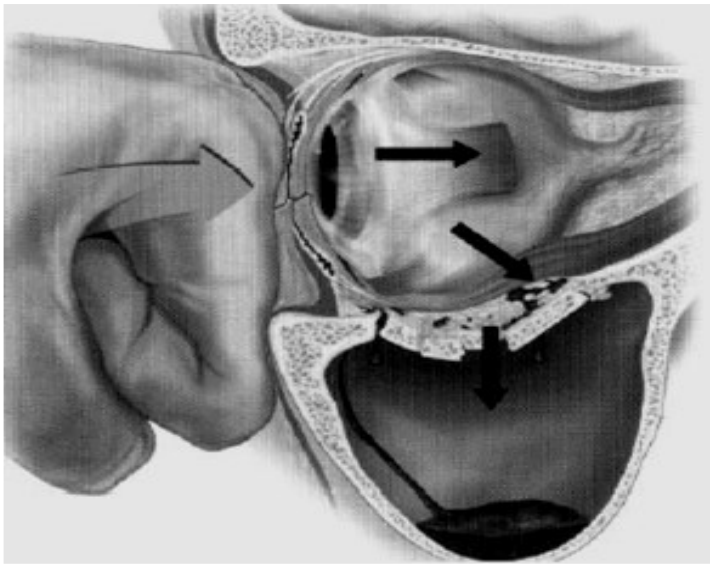

Figure 5: Mechanism of fracture of the orbital floor [22] (blow-out).

2.1. Symptoms of an eye socket fracture

The following assessments are characteristic of orbital floor fractures and mandate further imaging [28]:

1. *Diplopia (on upward gaze)*
2. *Limitation of upward gaze*
3. *Trigeminal function assessment: The infraorbital nerve runs along the floor of the orbit. decreased sensation over the inferior orbital rim, extending to the edge of the nose and ipsilateral upper lip.*
4. *Tenderness, or step-offs at the infraorbital rim*
5. *Subcutaneous emphysema (indicates a fracture of the maxillary sinus)*
6. *Oculomotor function: Entrapment of the inferior rectus muscle; often occurs between fragments of the lower orbit and is the cause of diplopia*
7. *Pupillary light reflex: An absent reflex can show damage to the afferent or efferent nerve system*
8. *Gross visual acuity*
9. *Position of the globe: A dislocated fracture can lead to enophthalmos and swelling behind the globe, to exophthalmos*
10. *Chemosis and sub-conjunctival haemorrhage*
11. *Edema and periorbital ecchymosis*

2.2. Treatment

Many clinicians have recommended that orbital volume increases be treated, as an indication for early reconstructive surgery. In general, surgery should be undertaken within 14 days to prevent fibrosis. Most surgeons wait 24-72 hours to allow the edema to subside before undertaking surgery. Patients with fractures where the orbital floor fragments are not displaced, and the orbital volume remains unchanged, can be addressed without any surgical intervention. In fact, the goal of surgery is to restore herniated structures into the orbital cavity. The surgery may be done via a transconjunctival or trans maxillary approach. Today there are endoscopic techniques to manage the orbital fracture. Several types of implants are also available for reconstruction of the orbit, but these should be avoided in the presence of an obvious infection [29].

3. literature review

The most important component of orbital reconstruction is restoration of the peritraumatic anatomy and volume of the internal orbit [30]. Computed tomography (CT) is the gold standard used for imaging diagnosis in orbital traumatology. Various materials are used for the reconstruction of orbital wall fractures. These include autografts, allografts, xenograft and metallic or non-metallic alloplastic bone substitutes and have yielded varying degrees of success [31]. Ethisorb® patch is a synthetic absorbable implant that was designed for the bridging of dura mater encephalin and spinalis defects. Mainly orbital floor has been reconstructed with titanium mesh and in related article adjusted with Ethisorb® patch (The absorbable material). Metallic meshes provide better stability for bone grafts and is reliable and accurate in the reconstruction of internal orbital defects. In addition, it possesses flexibility, which allows conformation and moulding, even to a complex bone contour, with no donor site morbidity. However, the main drawback of titanium implants is the risk of postoperative infection and/or extrusion. Ethisorb® is a well-known material used to close dural defects which causes a low rate of postoperative inflammatory reactions and adhesions and is an interesting material for use in the reconstruction of medial orbital wall defects. Ethisorb® patch is that it supplies an anatomically correct fit to the orbital medial wall but does not require fixation by screws or the use of sutures.

Furthermore, Ethisorb® is a cost-effective material as it costs significantly less than PDS foils or titanium mesh [32]. Preoperative conventional high-resolution computed tomographic (CT) data were used to create a virtual model of the ideal form of the affected orbit by mirroring the unaffected side using Materialise Mimics software. A preoperative solid model was then additive manufactured with 3D Printing. The design process of accurate bio-models of human anatomy and customized implants derived from medical image data of an existing tangible object according to a process known as reverse engineering [33]. Computer assisted manufacturing and Rapid prototyping (RP) processes follow in the physical, solid object production from the virtual CAD models using additive or subtractive technologies offering a wide range of materials such as plastic, metal, ceramics, powders, liquids, or even living cells.

Since their introduction in 1980, rapid prototyping techniques influenced more and more the biomedical field with different applications ranging from bio-printing tissues and organs to moulds for prosthetics and surgical guides, patient-specific implant up to drug-delivery devices and forensic science[34]. Additive manufacturing (AM) techniques otherwise known as three-dimensional (3D) printing, refer to the process of building a device by joining material layer by layer. Conversely to the traditional process of subtractive manufacturing [35] ,it starts from a CAD model decomposed into transversal sectional layers where virtual trajectories instruct the 3-D 'printer' where to deposit the layers of material through proper technologies such as: Selective Laser Sintering, Fused Deposition Modeling, Multi-Jet Modeling and Stereolithography. Five technical steps are required to finalize a printed model.

Briefly, AM include selecting the anatomical target area, the development of the 3D geometry through the processing of the medical images coming from a CT/MRI scan, the optimization of the file for the physical printing, and the appropriate selection of the 3D printer and materials (Figure 6).

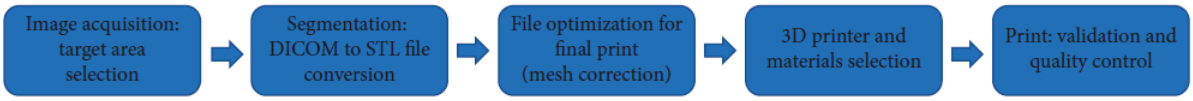

Figure 6: 3D-printing workflow.

Generally speaking, the potentials of AM span over different fields and entail a reduction in the time to market, reduction of cost development, customization of unique item and spare

parts, on-site and on-demand manufacturing (printing in remote locations by local distributors and service providers), quality improvement, smaller environmental footprint as only needed materials are used [36].AM Technologies can be categorized into seven different categories (Figure 7)

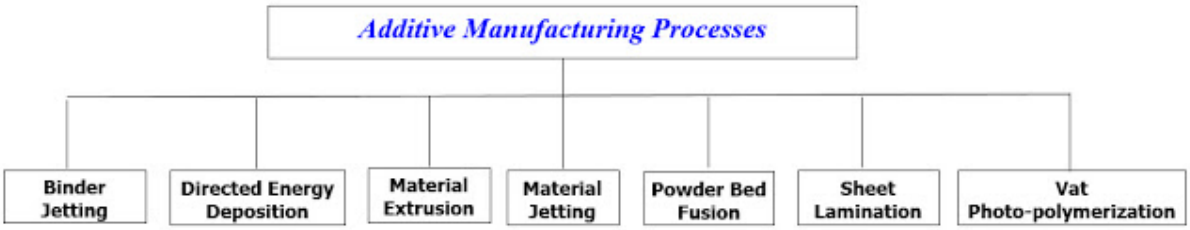

Figure 7: flowchart of AM Technologies

In fact, the 3D printing has been used in a wide range of healthcare settings including, but not limited to cardiothoracic surgery [38], cardiology [39], gastroenterology [40], neurosurgery [41], oral and maxillofacial surgery [42], ophthalmology [43], otolaryngology [44], orthopaedic surgery [45], plastic surgery [46], podiatry [47], pulmonology [48], radiation oncology [49], transplant surgery [50], urology [51], and vascular surgery [52].

Medical Rapid Prototyping can be applied to oral and maxillofacial surgery, dental implantology, neurosurgery and orthopaedics [53] with the following purposes:

- ***Bioprinting Tissues and Organs:** the current treatment for organ failure relies mostly on organ transplants from deceased donors or living matching donors. The chronic shortage of human organs available for transplant lead to the necessity of using cells taken from the organ transplant patient's own body to build a replacement organ hence minimizing the risk of tissue rejection and lifelong intake of immunosuppressants. Thus 3D bioprinting has been used for generating and transplanting different tissues including: skin, bone, vascular networks, heart tissues and organs [54] improving the traditional tissue engineering strategy requiring isolation of steam cells from tissue samples, multiplication with growth factors in laboratory and a highly precise cell placement onto scaffolds for cell proliferation. Thus, a high digital control of speed, resolution, cell concentration, drop volume, and diameter of printed cells allowed a better differentiation into functioning tissues.*

- ***Moulds for prosthetics and Surgical guides:*** *Historically, surgical guides and tools were generic devices made of titanium or aluminium. By implementing AM, physicians can create guides that precisely follow a patient's unique anatomy, accurately locating drills or other instruments used during surgery resulting in better postoperative results. Moreover, anatomical models of the diseased site and specific moulds based on the anatomy of the cranial defect to be repaired can be fabricated and used as guides to manufacture prostheses.*
- ***Customized Implants and Prostheses:*** *custom-made prostheses can be produced starting from MRI or CT scans converted into digital. stl (standard triangulation language) 3D print files modelled through computer aided design tools to full match the desired shape. In this way fabrication time, cost, surgery time, and post-operative complications are reduced.*
- ***Anatomical Models for Surgical Planning, Practicing and Education:*** *Having a tangible, realistic model of a patient's anatomy could be useful for the simulation of the surgery, but also for surgical training which basing on cadavers presents problems of availability and cost. Cadavers also often lack the appropriate pathology, so they provide more of a lesson in anatomy than a representation of a surgical patient.*
- ***Custom 3D-Printed Dosage Forms and Drug Delivery Devices:*** *the potential to produce personalized medicines such as pills that include multiple active ingredients or medications printed in one multidose form that is fabricated at the point of care can provide patients with an accurate, personalized dose of multiple medications in a single tablet to improve their compliance. Implantable drug delivery devices with novel drug-release profiles can also be created for a direct treatment towards a specific area saving non-affected tissue.*
- ***Forensic science:*** *allows for anatomically correct recreation of body injuries from CT and MRI scans to determine the mechanism of injury or to reconstruct the facial profile based on a 3D printed skull [34].*

The application of 3D printing in medicine can provide many benefits. The current work focuses on the development of a procedure to design a customized medical implant achieving the advantages (Figure 8).

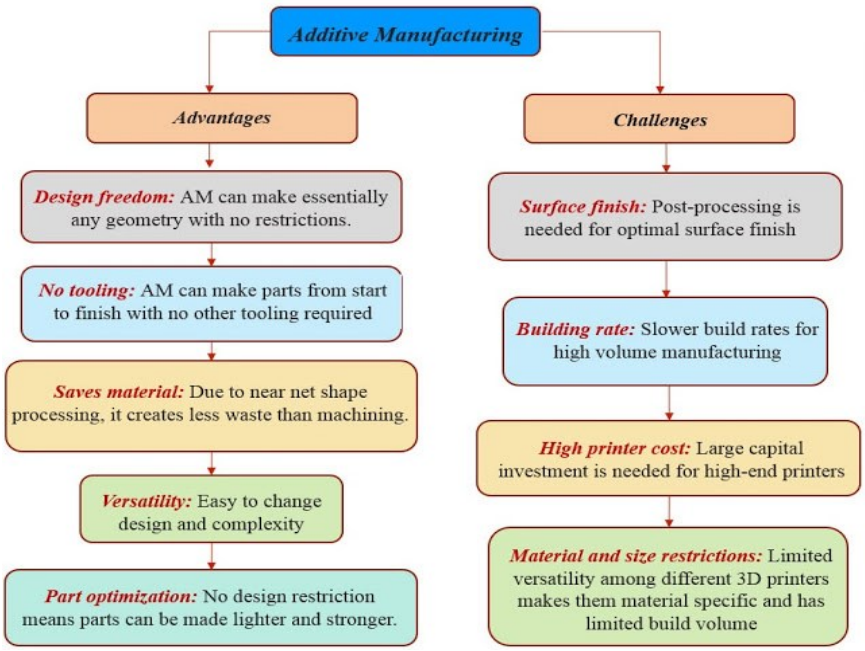

Figure 8: Advantages and Challenges in AM.

3.1. Additive manufacturing

The manufacturing processes include subtractive manufacturing, which cuts off a piece of material to form the final shape, and additive manufacturing, which builds up the material by stacking [59]. Subtractive manufacturing, the traditional machining technique has the disadvantage in that it is difficult to make complicated shapes by computer numerical control (CNC) milling and there is a lot of material waste [60]. Additive manufacturing, known as rapid prototyping or 3D printing, has the advantage of being very sophisticated, with less material waste, faster production times, and the ability to produce complex structures. There are various kinds of manufacturing processes. The manufacturing process should be selected with consideration of the material type, available technology, post-processing, accuracy, lead time, properties, and surface quality (Figure 9).

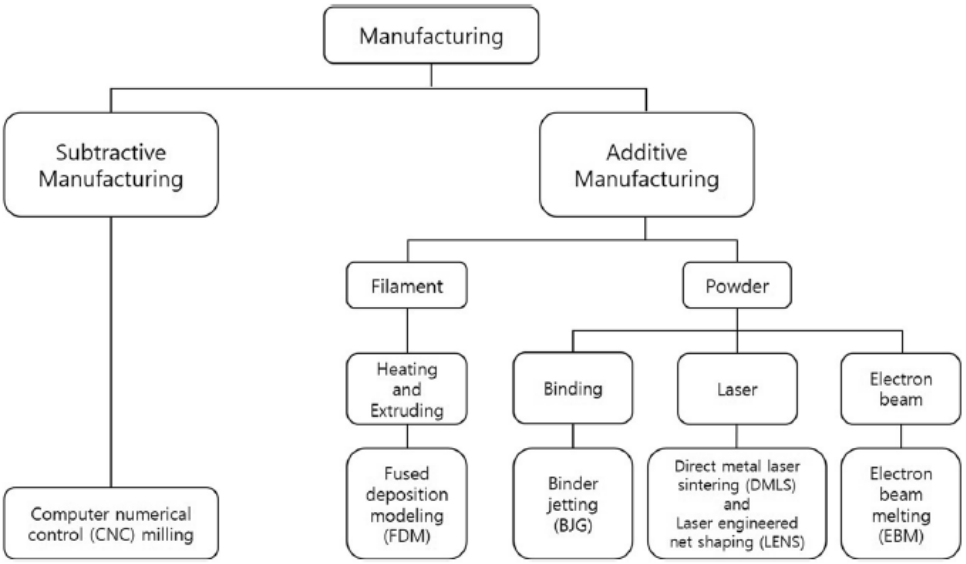

Figure 9: Schematic of the manufacturing processes [61]

3.1.1 binder jetting (BJG)

BJG generally uses two materials: a powder material from which the part is made and a binder material that bonds between the powder materials (Figure 10).It has the advantage that parts can be produced without support structures, but it has the disadvantage that post processing takes more time than actual printing, resulting in a significant increase in cost. In addition, the parts have rough microstructure and lower mechanical properties than those produced by selective laser melting (SLM) or EBM because of the possibility of porosity and heat treatment [68].

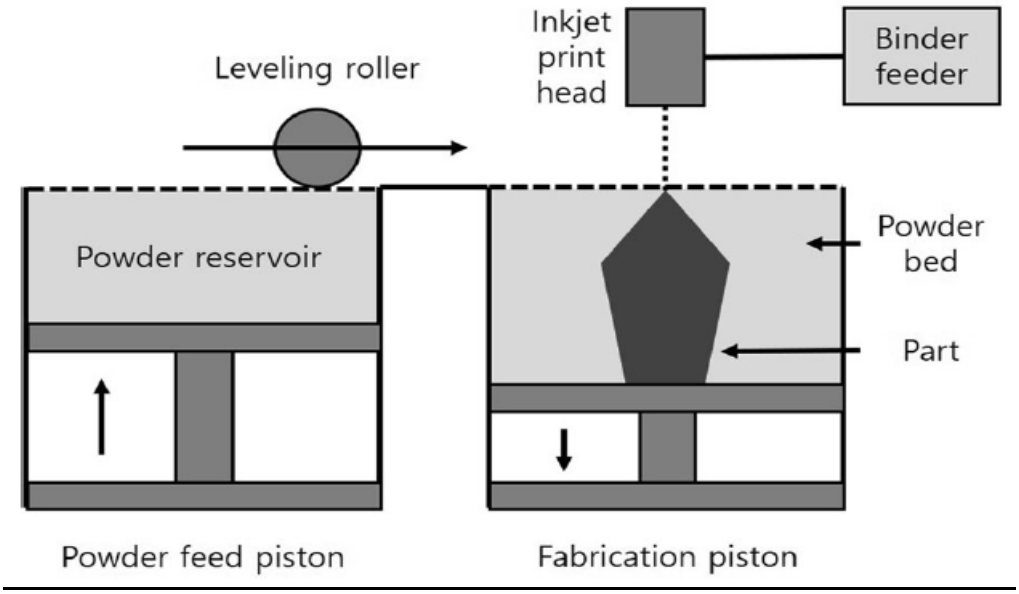

Figure 10: Binder jetting schematic

3.1.2 direct metal laser sintering (DMLS)

DMLS, referred to using the terms SLM or selective laser sintering (SLS), uses a high-powered optic laser to fuse the metal powder to solid components based on a 3D CAD file and, similar to EBM, is built layer by layer [69]. Like BJG, a powder bed is used to create a 3D object. However, instead of using a spray solution, a laser is used to tie the powder particles together, and the laser is instructed to draw a specific pattern on the surface of the powder bed during the printing process [70]. When the first layer is completed, the roller sprinkles a new layer of powder on top of the previous layer, pushes it flat, and then uses the laser to make the object layer by layer [71] (Figure 11). DMLS have many advantages and disadvantages [68]. The advantages include the use of a wide range of materials, improved functionality, relatively low cost, and the production of ready-to-use near-net shaped components. On the other hand, the disadvantages include relatively slow processes, size limitations, high power consumption, and high initial cost. In addition, the handling of the powder is tricky, the produced parts can have rough surfaces, and the brittle materials that cannot accommodate high internal stress during the manufacturing process can cause cracking of the parts.

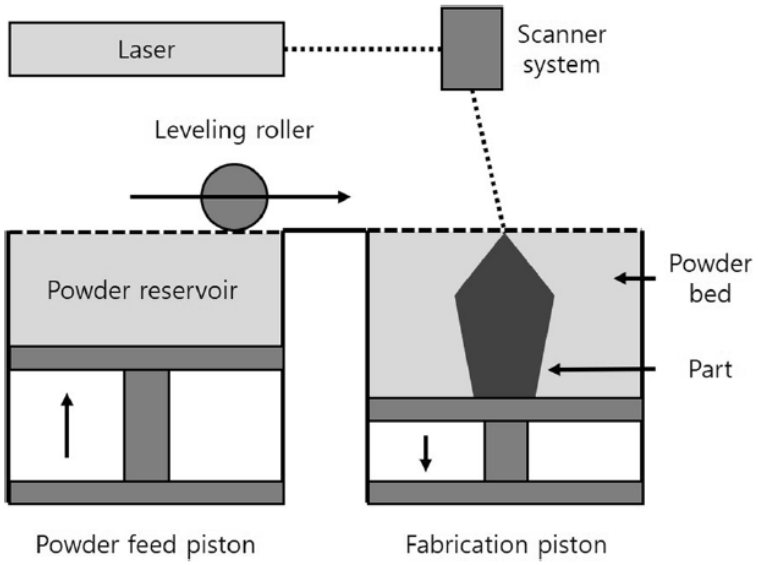

Figure 11: Direct metal laser sintering schematic

3.1.3 electron beam melting (EBM)

EBM is very similar to DMLS, but there is a slight difference in that the parts are fabricated by melting the metal powder in a layer using an electron beam [69] (Figure 12). In EBM, the cooling rate can be greatly reduced by increasing the temperature of the powder bed. Unlike DMLS, EBM has the ability to treat brittle mate-

rials that cannot be processed by DMLS because it slowly cools, avoiding solidification cracking of brittle materials. However, it takes longer than DMLS and requires sufficient cooling time before removing parts from the substrate plate because the electron beams are used many times in the layers [68].

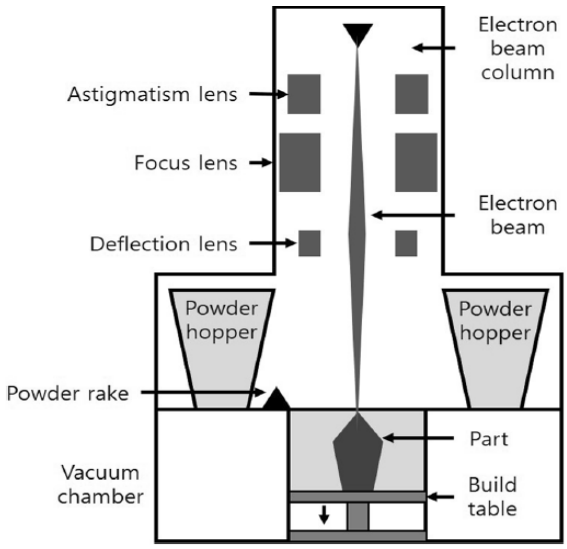

Figure 12: Electron beam melting schematic

3.1.4 laser engineered net shaping (LENS)

Similar to EBM and DMLS, LENS is used to fabricate metal parts directly from CAD solid models and has the difference in that metal powders are injected into the molten pool generated by the condensed high-power laser beam [69]. The molten material line rapidly solidifies as the laser beam retreats, and after each layer is formed, the laser head advances by one-layer thickness together with the powder feed nozzle, and a subsequent layer is created. This is repeated several times until the entire object displayed in the 3D CAD model is created [72] (Figure 13).

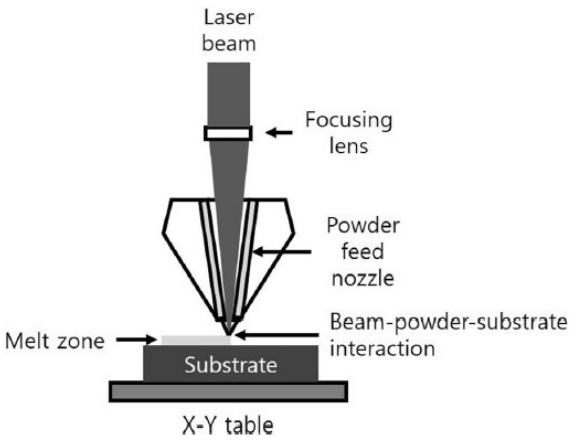

Figure 13: Laser engineered net shaping schematic

3.1.5 fused deposition modelling (FDM)

FDM is generally carried out with a polymer melted in a printer nozzle and arranged layer by layer. The material is melted and deposited at a defined location on the printing layer, and after the first layer is completed, the distance between the printing bed and the extruder nozzle is increased and the second layer is printed on the first layer [72] (Figure 14).

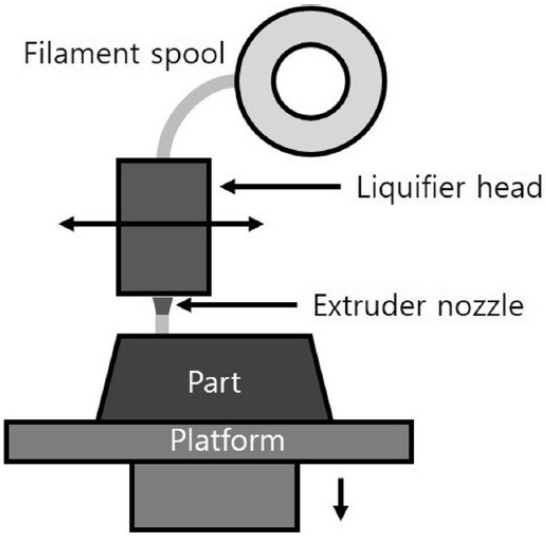

Figure 14: Fused deposition modelling schematic

3.2. Implant materials

The ideal material is biocompatible, easy to shape, high strength, non-toxic, inexpensive, durable, radiolucent, and lightweight [62]. Materials include non-resorbable materials such as titanium, polyethylene, polyether ether ketone (PEEK), and hydroxyapatite (HA) and absorbable materials such as poly-DL-lactic acid (PDLLA), polylactideco-glycolide acid (PLGA), and calcium phosphate.

Titanium is the metal of choice for manufacturing implants. It has the advantages of high strength, biocompatibility, lightweight, corrosion resistance, and the potential for osseointegration [63]. However, it has the disadvantage of causing scatter artifacts in CT scans [64]. Polyethylene includes porous polyethylene (PPE) and ultra-high molecular weight polyethylene (UHMW-PE). PPE such as Medpor was used for reconstruction of the orbital floor and augmentation of the facial area [65]

Titanium is the metal of choice for manufacturing implants. It has the advantages of high strength, biocompatibility, lightweight, corrosion resistance, and the potential for osseointegration [66]. However, it has the disadvantage of causing scatter artefacts in CT scans [67].

porous polyethylene (PPE) was used for reconstruction of the orbital floor and augmentation of the facial area because of easy to shape but there is a possibility of infection.

UHMW-PE can have a lower infection rate than PPE. Polyethylene has the advantage of not producing artefact because of radiolucency in CT, but it also has a disadvantage that it is difficult to control implant position after surgery.

PEEK has similar strength and elasticity to bone and is easy to modify.It is radiolucent in CT and offers more comfort to patients, with lower thermal conductivity and lighter weight than titanium. However, it had reports of infection and foreign body reaction.

HA is osteoconductive and non-resorbable with a strong capacity to bind both hard and soft tissues but difficult to make complex shapes.

Calcium phosphate implants have been used have good biocompatibility and suitable biodegradation and are like the mineral phase of the bone, so they do not cause artefacts or interference seen in other metallic in CT or MRI. In addition, calcium phosphate implants show less mechanical performance than titanium but are suitable as a scaffold for bone tissue growth and can be loaded with bioactive protein or antibiotics.

3.3. Clinical application

During the surgical the patient-specific custom-made orbital reconstruction implant was placed onto the inferior orbital wall and fixed to bone with two screws. The surgery took about30 min. Normally this kind of surgery takes approximately 45 min when reconstruction plate is manually formulated during operation. The immediate outcome was successful, and the implant fitted precisely onto the ragged orbital wall.

4.MATERIALS AND METHODS

4.1. Data- eyeball Implant Modelling techniques

The 2D image data coming from MRI and CT scan are acquired in digital imaging and communications in medicine (DICOM) format. The data derived from the CT scan represent each point as an ordered triple (x, y, z) in a given reference system in order to define the surface geometry of the CAD model either in non-uniform rational B-splines (NURBS) or STL (triangular mesh) format. The DICOM data is then processed using software as MIMICS (Materialise, Belgium), to create a 3D model of the anatomy depicting the defect. The 3D model file is then imported into a design software (SolidWorks or Rhinoceros) to create the final implant design ready for additive manufacturing. The conversion of the 3D files to STL format, performed by biomedical software, generates a mesh of triangles, so that it can adequately represent the complex topography of the craniomaxillofacial region [33].The patient was a male who had orbital floor fracture. For treatment it has been decided to create a digitally designed and AM'd patient-specific alloplastic implant to achieve anatomically correct shape of the orbital wall and appearance of the eye symmetry (Figure 15).

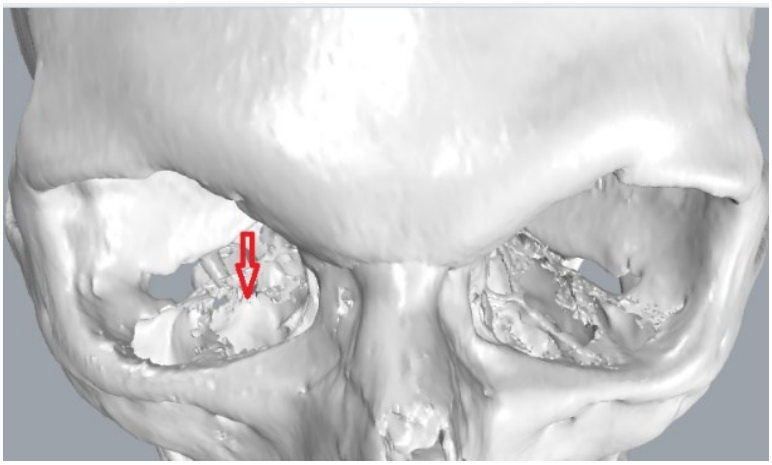

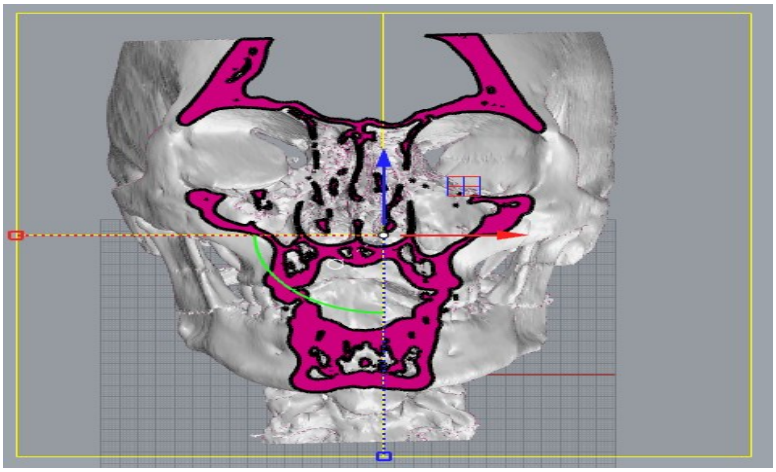

Figure 15: The computed tomography (CT) image of the orbital floor fracture is shown in Rhinoceros 6 software. defect of the entire orbital floor of left eye.

4.2. Modelling the implant

Traditionally, implants have been manually bent and shaped, either preoperatively or intraoperatively, with the help of anatomic solid models. But designing implant with Grasshopper software obviates the manual procedure and may result in more accurate and cost-effective implants [55]. The geometry of the orbital implant can be created by mirroring the shape of the facial structure from the opposite side and repositioning it to the actual side. Surface modelling of the implant was done using Rhinoceros 6.28 modelling software (McNeel an American company) (Figure 16). In order to be able adjusting different parameter of implant such as precision and number of control points and contours the parametric modelling is done in the Grasshopper Plugin which runs within the Rhinoceros 3D computer-aided design (CAD) application. Rhino software has application for drawing complicated curves and surface which works with NURBS and it has 3D modelling environment which it has command windows for typing different commands and it has 4 different viewport and toolbar (Figure 17).When install Grasshopper plugin in Rhino and type command 'Grasshopper' it will open the canvas of Grasshopper (GH) (Figure 18) and modelling in the GH is only based on algorithm. One interesting point about this plugin is that it has open source platform it means that it is possible to easily add or eliminate components and also ourself could produce new plugin in this environment (At present GH has nearly about 260 plugins! And all the plugins

name is get from name of animals) because of this various kind of plugin it made the GH environment as interdisciplinary environment such as modelling architecture, electrical modelling, robotic, mechanical, biomedical and other field .Also it is possible to connect GH to physical models and use the components base on our data. There is component pallet area that organizes components into categories and sub-categories (Figure 19).

In this project algorithms are implemented basis of CT scan image. Each component of GH has capability to accept some input and give the result. Flowchart for virtual parametric reconstruction of orbital floor is as follows: (1) apply imaging and acquire 3D visual models the healthy orbital cavity (2) this volume has been mirrored on the pathological side through the Mimics module (3) designing of implant on the basis of this acquired volume. The 3D visual model of the obtained mirrored healthy orbital cavity has been converted in standard (.stl) format for modelling of the surface. So, the .stl files containing the meshes of the pathological orbital cavity and of the mirrored healthy one has been imported in Rhinoceros 3D v.6.28 by McNeel Inc., that directly provide outputs .stl files for 3D printers and rapid prototyping systems [55]. Creating an editable NURBS surface from complex scan data can be a challenging proposition, especially when the original scanned surface is irregular and not smooth in the conventional sense. In the following focus on workflow that allows an editable surface to be produced whilst maintaining the irregular qualities of the target surface the workflow as described attempts to find a balance between the irregular target and the well-structured Rhino surface[56].The workflow as described is suitable for a variety of scenarios in different field of eyeball fractures and different patient (Figure 20).

***Open** a new Rhino file - choose **Small Objects Millimetres** from the template options.*

***Import** the STL data into Rhino - **File > Import** (choose STL from the Files of Type dropdown menu) and navigate to your STL file.*

*If the scanned data needs to be reoriented in 3D space this can be done with the **Transform** tools for instance **Transform > Move** or **Transform>Rotate**. It is important to carry out any reorientation of the model before work begins. The scanned data should come into Rhino's Default Layer -and then start **Creating the Contour Curves** for the layer of **mirrored orbit**.*

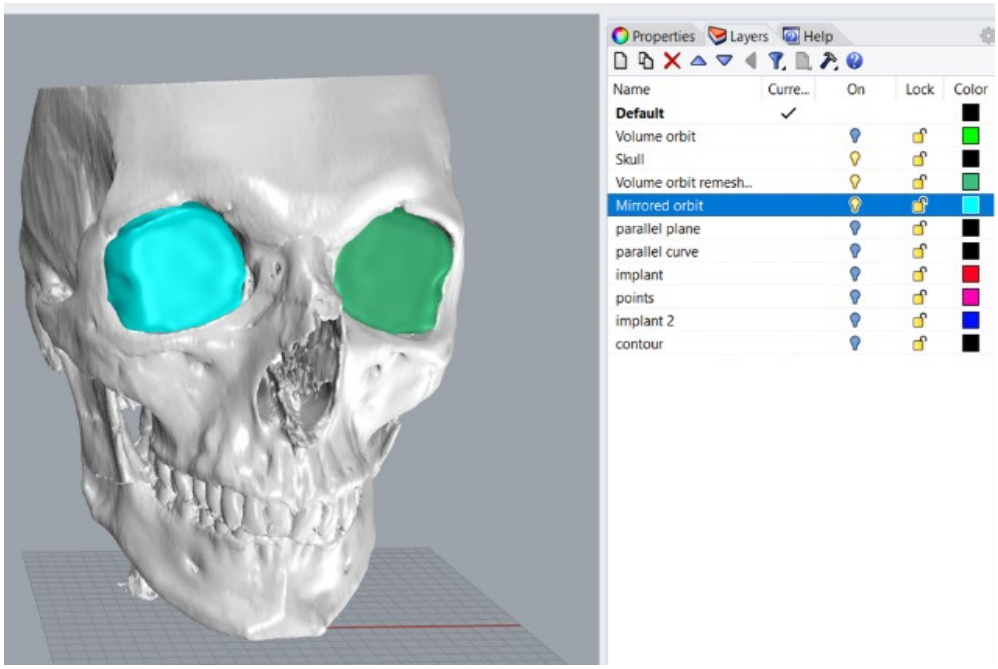

Figure 16: Healthy and mirrored orbital cavity 3D shape.

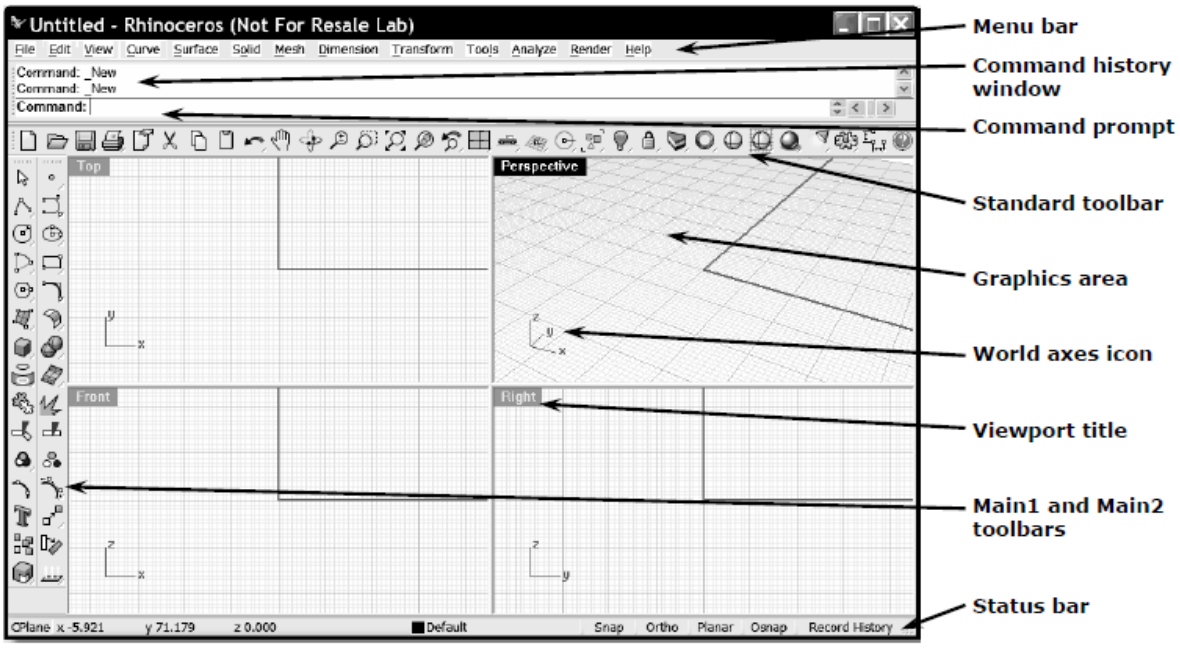

Figure 17: Rhinoceros environment

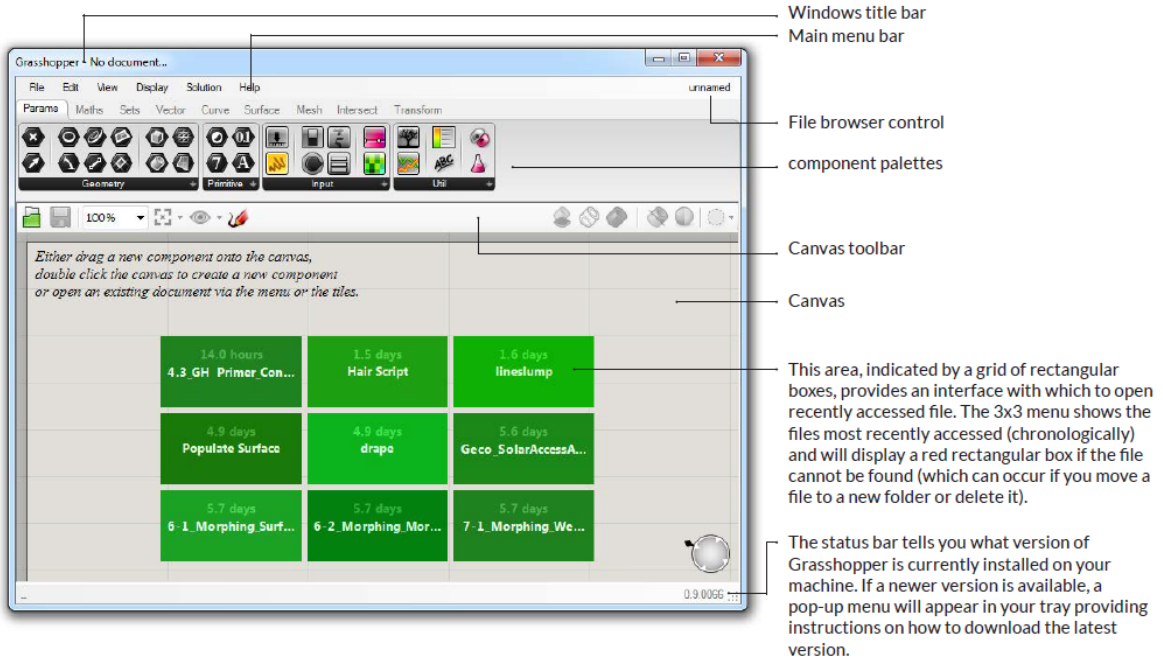

Figure 18: features of the Grasshopper environment

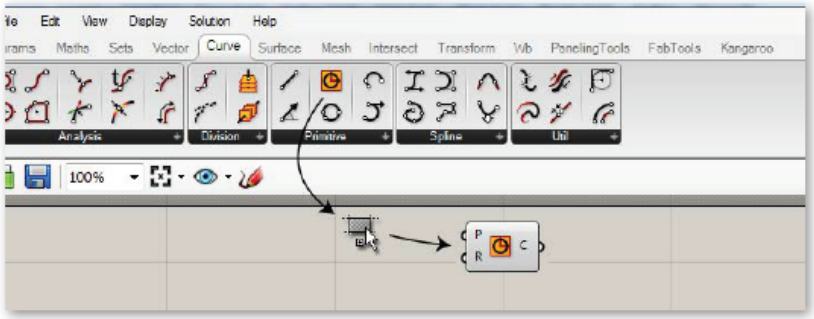

Figure 19: add a component to the canvas. It is possible either click on the objects in the drop-down menu or you can drag the component directly from the menu onto the canvas.

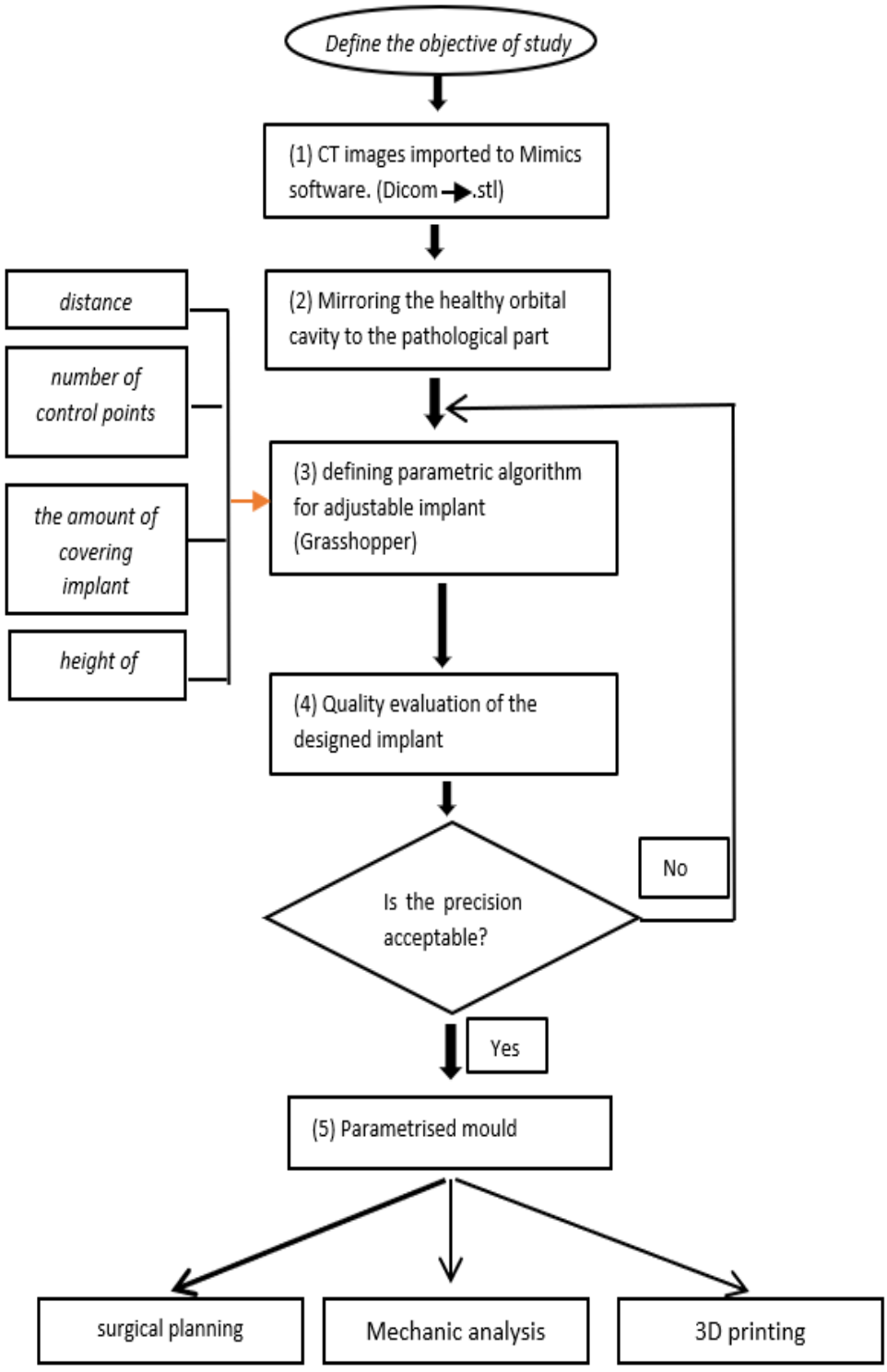

Figure 20: Flowchart for reconstruction of orbital floor

So, All the procedure has been developed using the commercial 3-D modelling software Rhinoceros version 6.28, developed by Robert Mc Neel & Associates. It focuses mainly on non-uniform rational B-splines (NURBS) mathematical model that allows to accurately represent curves, surfaces, solids, free form shapes. The sagittal plane corresponds to the symmetry plane dividing vertically the skull in two corresponding symmetric sides.

To define the Sagittal plane three bony unpaired craniometric landmarks have been selected in a way to be far enough to reduce the error in the alignment (Figure 21).

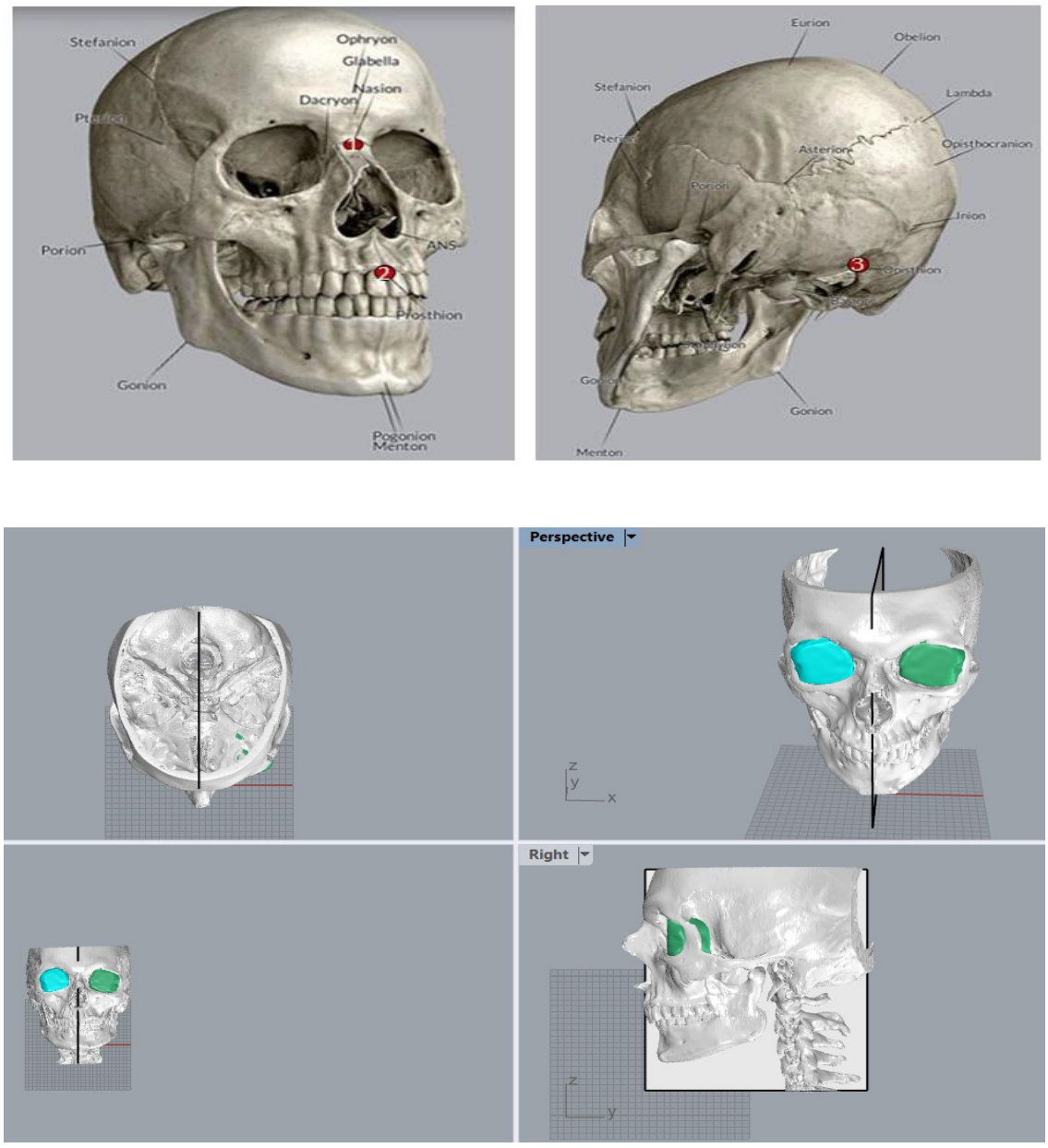

Figure 21: Cranial landmarks used to define the midsagittal plane: nasion (1), prosthion (2) and opisthion (3)

This chapter presents the theoretical foundation of parametric design for design generation of orbital implant and related mould that encompass the implant. Parametric design originates from generative design, which is a typical computational design approach based on rules or algorithms. This chapter starts with a critical review of generative design that is a general term commonly used to describe a number of computational methods that aim to automate the whole, or a part, of the design process. This is usually realized through rapid prototyping, powered by computers [74]. Grasshopper is a graphical algorithm editor that is integrated with Rhino3D's modelling tools. Grasshopper is used to design algorithms that then automate tasks in Rhino3D (Figure 22).

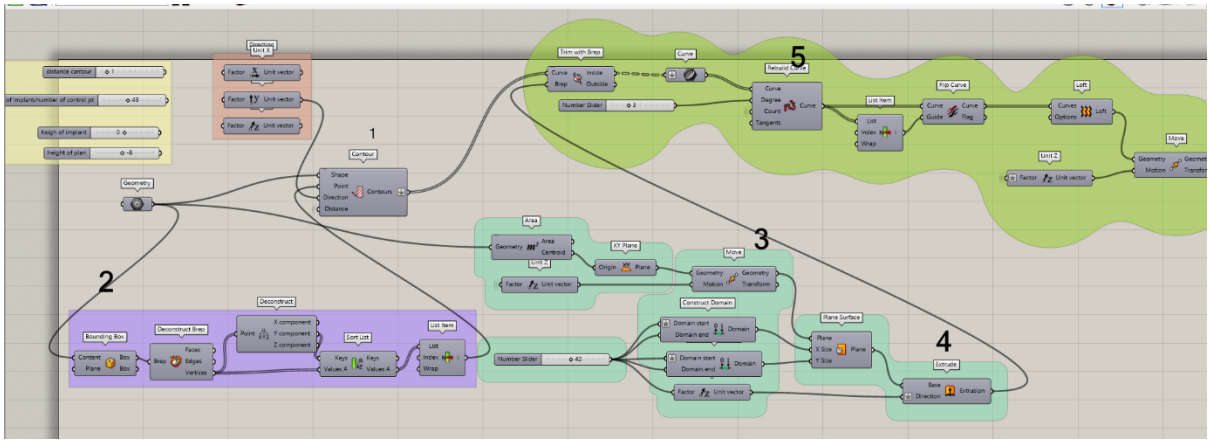

Figure 22: different groups of algorithm modelling of implant

Grouping components together on the canvas can be especially useful for readability and comprehensibility. Grouping allows you the ability to quickly select and move multiple components around the canvas (Figure 23).

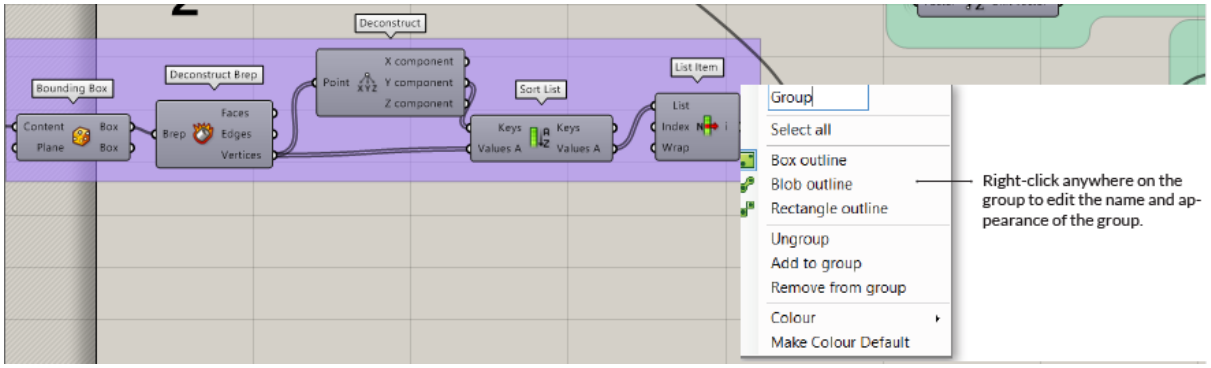

Figure 23: Method of Grouping in Grasshopper

Steps of parametric modelling is as follow:

1-Choose the total volume of the mirrored mesh as input of modelling and consider it in the close box and start contouring in different direction and determining the distance between contour (one way to control the precision of the implant) (Figure 24). In some circumstances it may be beneficial to produce contours further apart than 20(mm). The resulting contours are Polylines and will need to be Rebuilt to create smooth splines from which an editable surface can be created. Grasshopper allows to create visual programs called definitions. These definitions are made up of nodes connected by wires. Grasshopper consists of two primary types of user objects: parameters and components. Parameters store data, whereas components perform actions that result in data. Parameters store the data - numbers, colours, geometry, and more - that we send through the graph in our definition. Parameters are container objects which are usually shown as small rectangular boxes with a single input and single output. We also know that these are parameters because of the shape of their icon. All parameter objects have a hexagonal border around their icon. For example, parameter ***geometry*** *which contain the whole volume of orbital that represent a* collection of 3D Geometry (Index A.0). You can also Internalise data in a component input. Once you select Internalise data in the menu, any wires will disconnect from that input. The data has been changed from volatile to persistent and will no longer update. Components perform actions based on the inputs they receive. There are many types of components for different tasks (Index A.1). For this part **contour component** is used (Figure 24). Components are the objects you place on the canvas and connect together with Wires to form a visual program. Components can represent Rhino Geometry or operations like Math Functions. Contour component has four input (Shape, point, direction and distance).for the shape it is connected to the internalised parameter of geometry then for points it is defined the number of point with group 2 (Figure 24) (purple group) after that for direction consider different direction in (X , Y, Z) and finally for distance defined slider which determine the distance of contour in other word the precision of implant.

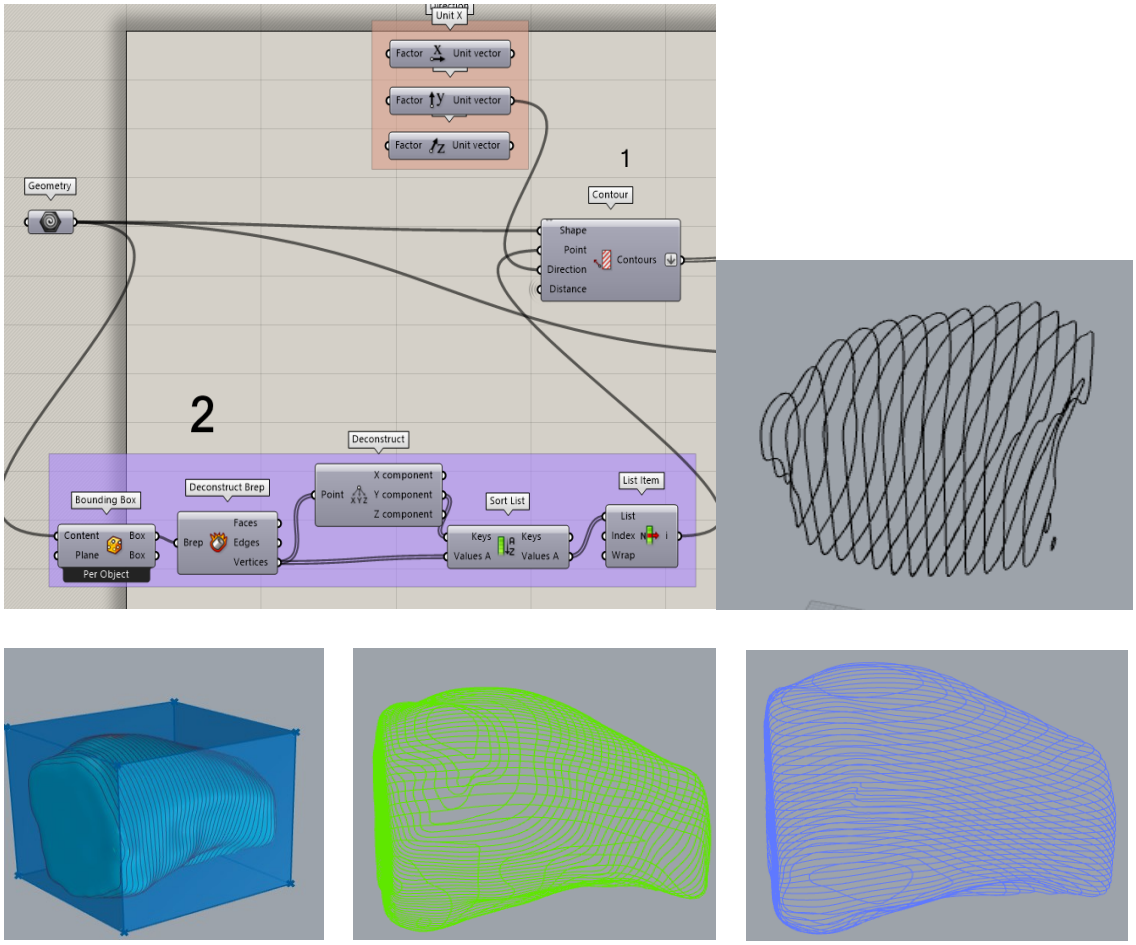

Figure 24: Contour component feature and the result and *Contouring in different direction of X-Y-Z*

For defining multiple points use component **list item** and **Sort list** Then **deconstruct** the points to find the positions of points and represent the border of these points with a **bounding box** which include the toral geometry (Index A.1).

It is important to remember that the output of contour must be Flatten (convert multiple sets to one set) for achieving the better result.

*2-For defining the surface of implant introduced a plan in which the height of it is adjustable (in direction Z) and then make it extrude (Figure 25).In order to define a plane that interrupt the contours use component **Plane surface** and determine **domain** in direction of (X, Y) that this plate has capability to **move** in direction of Z (Figure 26).*

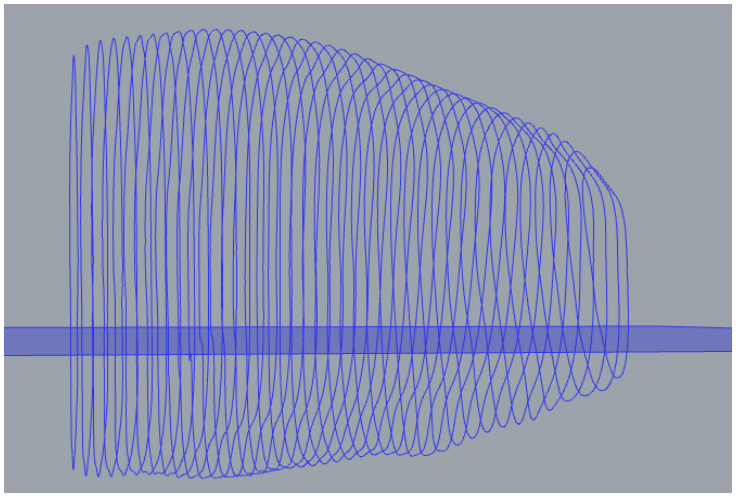

Figure 25: Height of plan

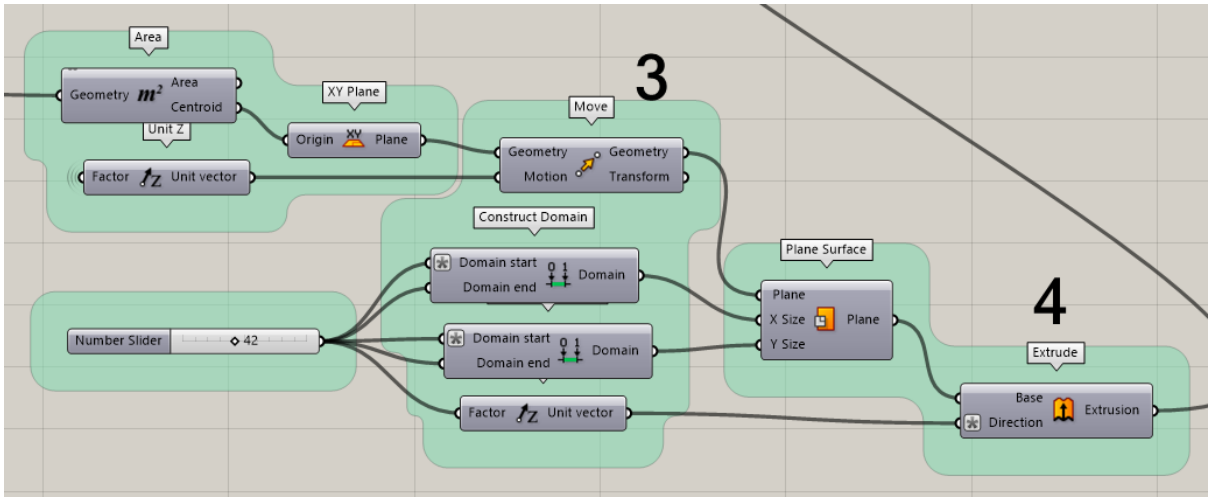

Figure 26: modelling algorithm of defining plane surface

*3-After that use, the components of **Trim**, **rebuild** (with changing the number of points it is possible to increase the precision) and **loft** for creation the floor of the implant. In other word Join the polyline segments and repair curve together to form one polyline. The completed contours should look like this (Figure 26). Then Rebuilding the Contour Curves and a rebuilt curve will deviate from the original polyline – it is possible to check this deviation by using the '**custom Preview**' component. As a general rule the more points in the rebuilt curve the closer it will be to the existing polyline but the more complex surfaces created from it - the aim is to reduce complexity whilst getting close to the original polyline. The rebuilt curves should look like this (Figure 27):*

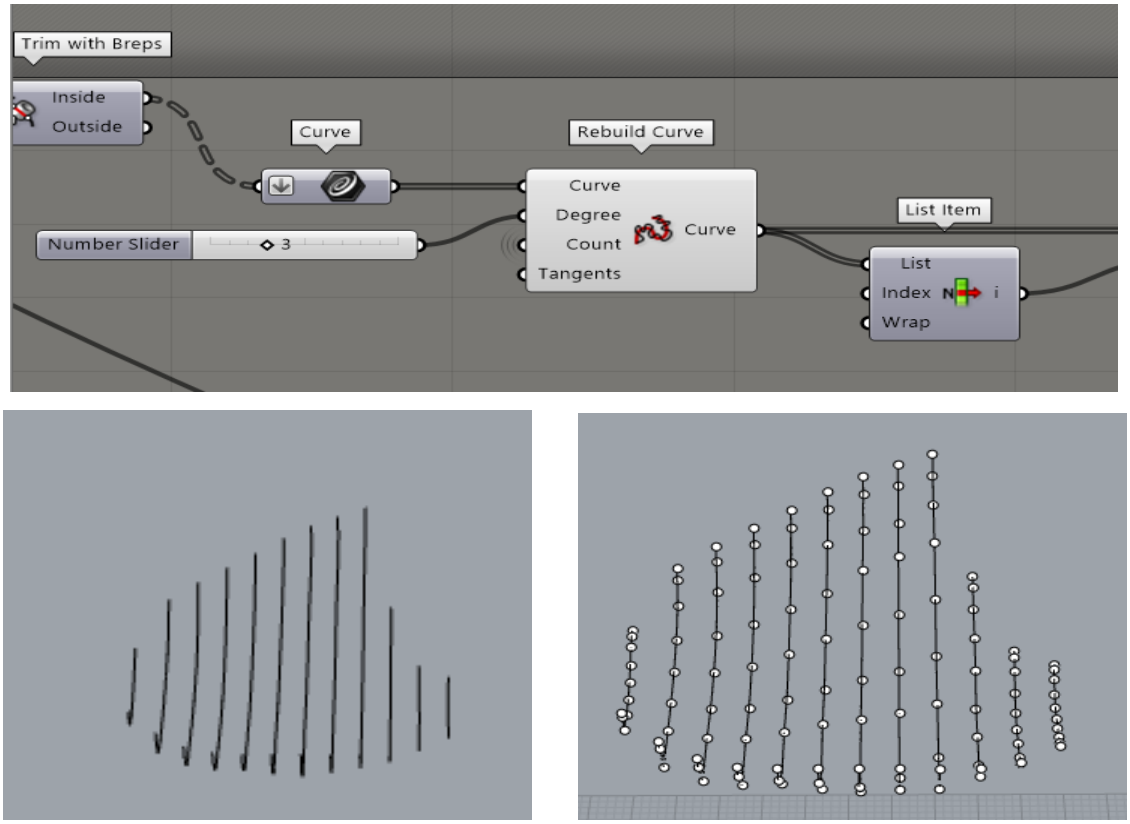

Figure 27: rebuilt curves

In this instance we need to create a surface that can be edited easily. Surfaces can be directly edited by their control points; however, in this instance the surface we will create will be relatively complex and have too many control points to edit it smoothly. for creating surface, the ***'unsplit loft surface'*** *component (*Represents a collection of Integer numeric values) *is used , and the result will be like (Figure 28).For obtaining a single continues surface it is better to use* ***unsplit loft surface*** *instead of* ***loft*** *comment which produce some fragmented surface as output .* It give as input a *Set of section curves or surfaces to loft through and Resulting untrimmed single unsplit lofted surface When you bake this surface into Rhino it will become a usual poly surface (Brep).This component is selected from pufferfish plugin (index A.2)(download it from food4rhino site and install it).*

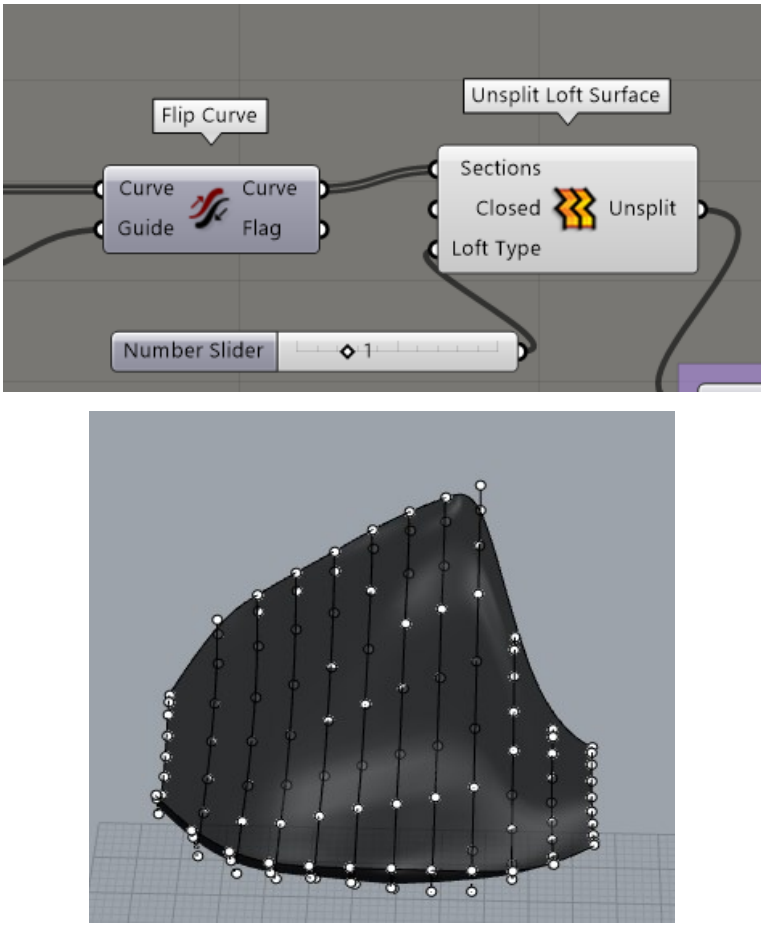

Figure 28: Unsplit loft surface of implant

*For attain better result before making loft we used **flip** component to make all the normal vector in the same direction (index A.1).*

*AT the final step add the capability for moving the implant in direction of the Z with the component '**move**'.*

In this algorithm it is possible to change four parameter such as distance contour, number of control points, the amount of covering implant of eyeball and height of implant [56] (Figure 29).

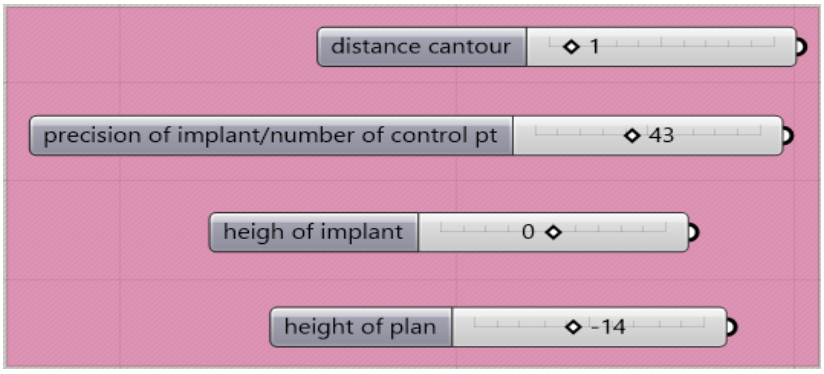

Figure 29: Parametric modelling of implant with option of controlling different parameters of implant rapidly.

Totally for planning eyeball implant should consider several aspects such as the amount of covering the implant on the basis of kind of fracture and the location of problem(Figure 30) secondly The shape of the implant should be accurately evaluated to warp the implant to the region of the skull defect. The fixation type is another important issue to avoid loosening of the implant. Loosening of an implant in situation can create specific wear, called fretting which can eventually fail the implant [57]. To secure the implant plates or screws of proper dimensions can be used according to the material type. Fixation can also be improved by proper osteointegration of the implant with the bone. A biomimetic approach coupled with bone tissue engineering techniques help tissue formation by supporting nutrition transport and delivery thus inducing bone regeneration [58].

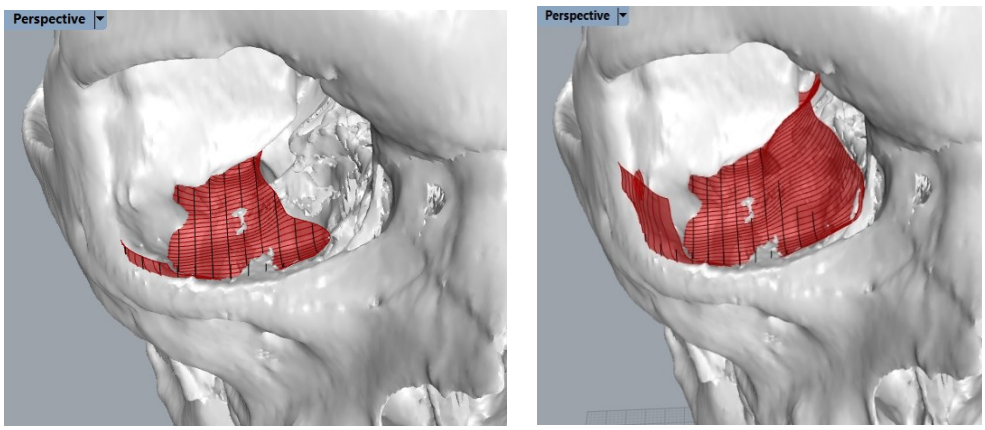

Figure 30: control digitally the amount of covering the implant the eyeball surface

3.3. Modelling the mould

The implant has been proposed under the guide of a mould. The mould has been designed by using Rhinoceros v.6.28 by McNeel Inc. that encompass the designed implant in the previous step.

For this purpose, the parametric modelling has been done in Grasshopper. The input of the mould design process is the implant modelled through the previous steps, but first its quality and accuracy must be verified. The mould must satisfy several technological and clinical needs to prevent issues with the 3D printing technology and to be successfully used during surgery.

In this part with this algorithm there is capability to control different parameters such as the dimension of mould, the radius of fillet and the distance of pins and etc figure.

In this part the goal is to improve the moulding effect by projecting the upper and lower template body of it which will be exactly fixed to the designed implant. (Figure31) presents the 3D geometry of the mould. The picture shows the nomenclature of the mould features.

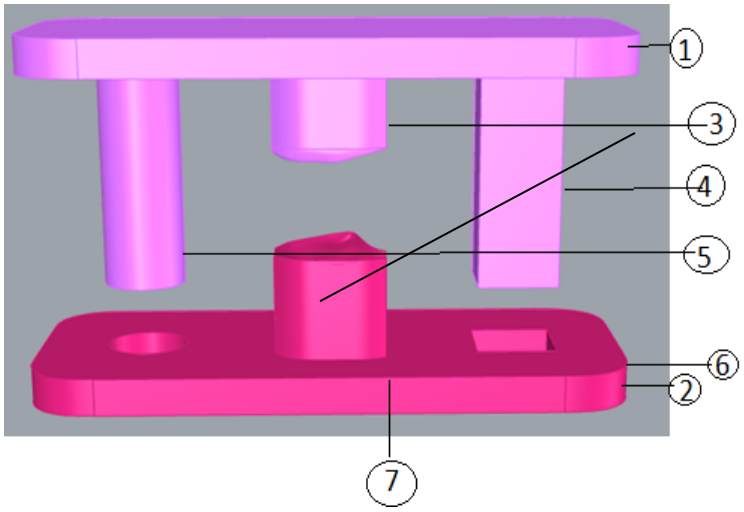

N.	Feature
1	Punch
2	Die
3	Active surface
4	Pin
5	Cylinder
6	Reference
7	Thickness

Figure 31: nomenclature of the mould features

Die and punch's shapes have been defined to improve the mould usability. The upper surface of the die has been constructed by projecting of implant boundaries along the directions perpendicular to the extracting one, thus obtaining a large square base. This solution ensures a large contact area to improve stability during the mould usage.

The lower surface of the punch has been constructed moving the Die part in direction of opposite on base of height of projection. In this manner, once closed the mould,there will be enough space for the surgeon to trim the unmodelled side areas of the implant. The upper surface of the punch has been designed to reduce the material consumption as much as

possible [55]. The mould guarantees a vertical gap of 1 mm between the pins and relative cylinders for modelling implants with different thicknesses. The distance of pins is adjustable which has been determined guaranteeing the possibility to insert the undeformed implant. For this part again use different components related to modelling mould and then make them as groups for better understanding (Figure 32). In continue describe the methods step by step.

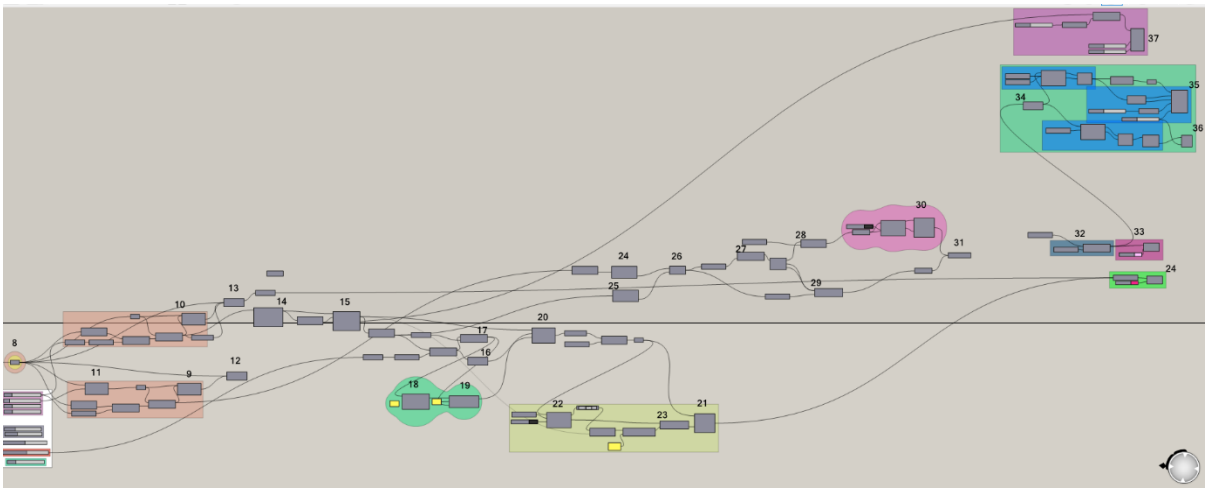

Figure 32: Modelling algorithm of mould

Steps for designing mould is as follow:

1-The mould algorithm start from getting the output of the previous section as an input for modelling and project the surface of implant on the curve (Figure 33). with ***project*** *component Project an object onto a plane. This option get geometry and plane as input and give geometry and transform as output. In fact, provide perimeter of our implant then with* ***unsplit loft surface produce*** *a continues surface and with* ***planar surface*** *Create planar surfaces from a collection of boundary edge curves.*

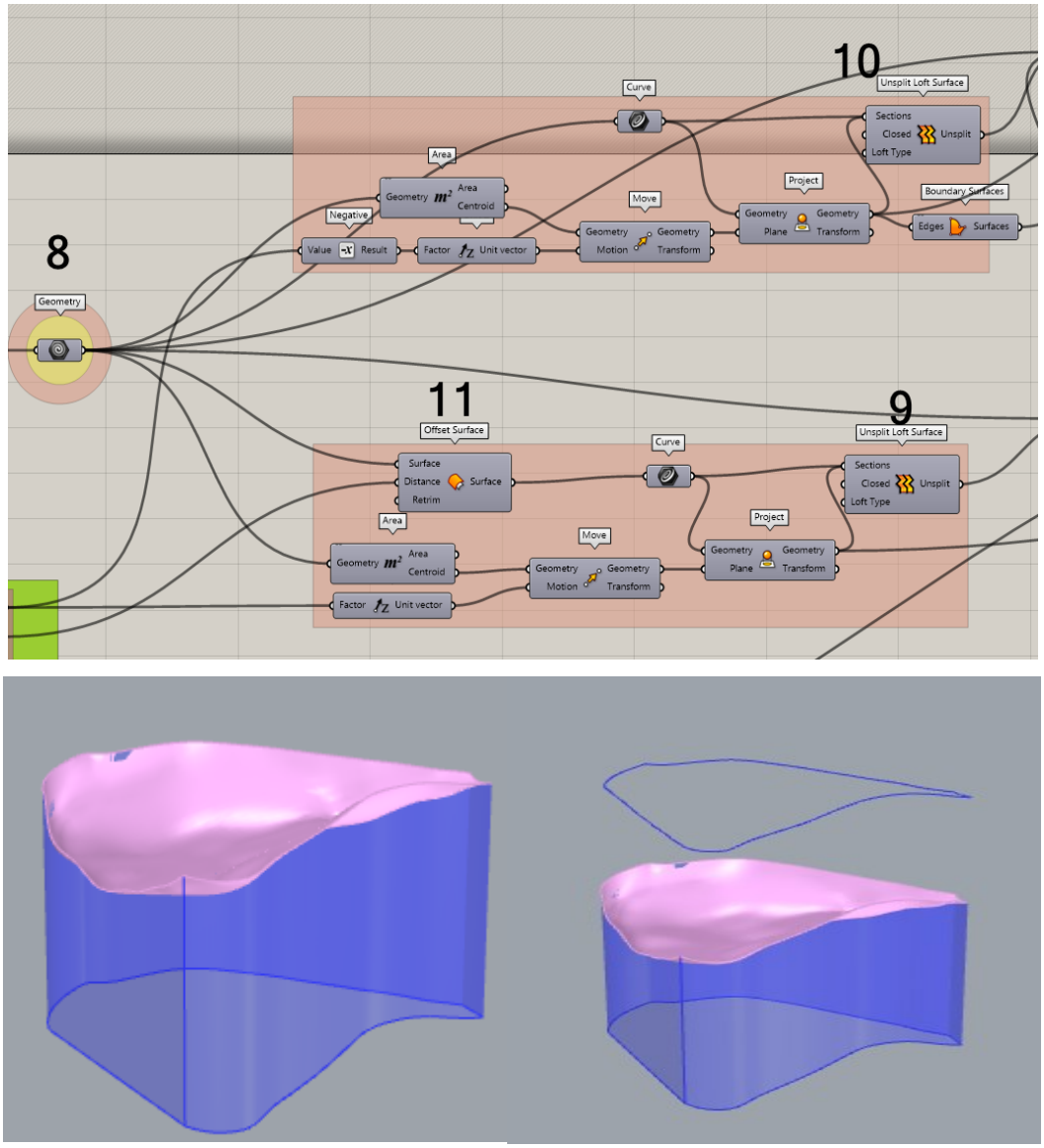

Figure 33: Projecting the surface of implant as curve in which the height of projection is possible to change

2-Considering a Gap (as component offset) between the implant and the upper side of mould (Figure 34) that Offset a surface by a fixed amount. As input get base surface and Offset distance (Number) as out give Offset result.

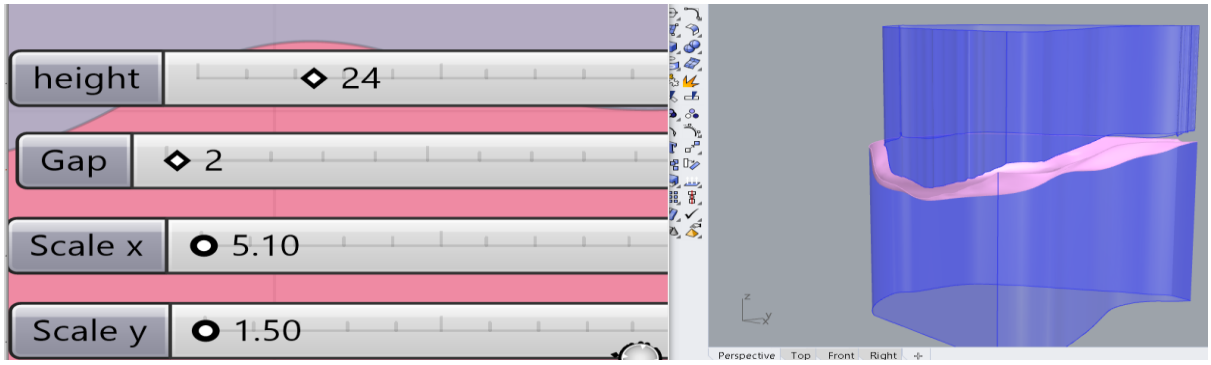

Figure 34: determining gap distance

*3- with component **'bounding rectangle** 'draw a rectangle which include the perimeter of implant (Figure 35). Create a plane-oriented union bounding rectangle or separate bounding rectangles for geometry. This component is chosen from pufferfish plugin (Index A.2).it has superiority respect to the rectangle component of the default which able to accept geometry as input. With component **Scale NU** control the edges of the base plate (Table 1).*

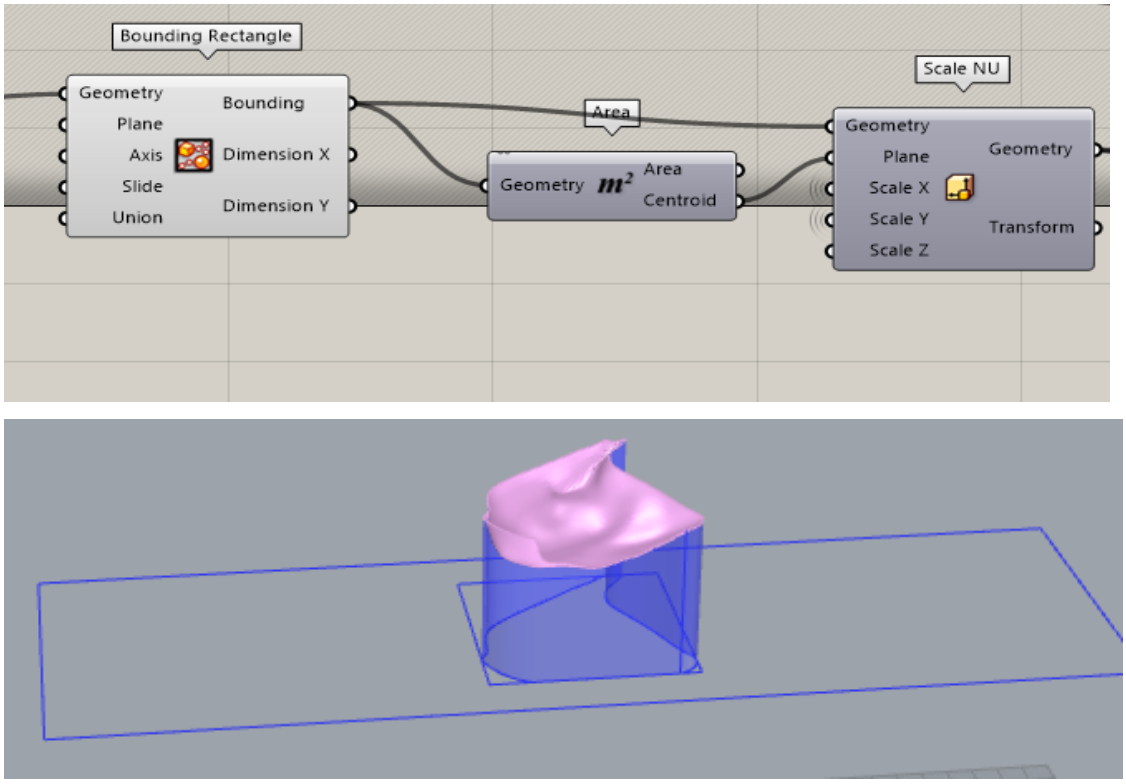

Figure 35: Adjustable base plate

Inputs

Name	ID	Description	Type
Geometry	G	Base geometry	Geometry
Plane	P	Base plane	Plane
Scale X	X	Scaling factor in {x} direction	Number
Scale Y	Y	Scaling factor in {y} direction	Number
Scale Z	Z	Scaling factor in {z} direction	Number

Outputs

Name	ID	Description	Type
Geometry	G	Scaled geometry	Geometry
Transform	X	Transformation data	Transform

Table 1: Scale NU component

4-Consider the centre of base plate (XY plane) and draw the adjustable rectangle and circle (the pins) (Figure 36).with component of ***circle*** *draw a circle and* ***mirror*** *the centre of this circle to other side for drawing centre of rectangular pin.* For drawing rectangular edge *use* ***polygon*** *component that make it possible to control the number of desired pin (Figure 37) (e.g. 4 or 6 or more than edge) that here we choose 4 and after that rotate it 45 degree to create a square (Table 2).*

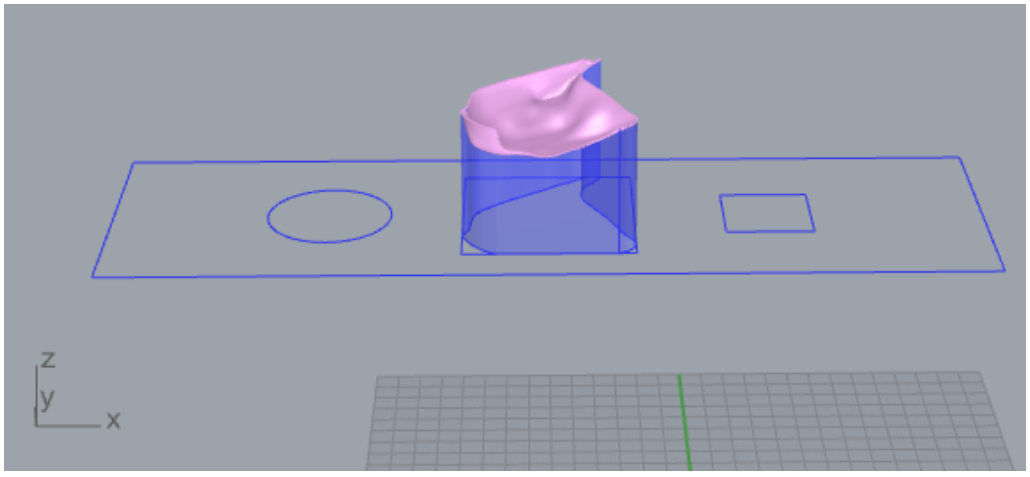

Figure 36: Adjustable pin plate

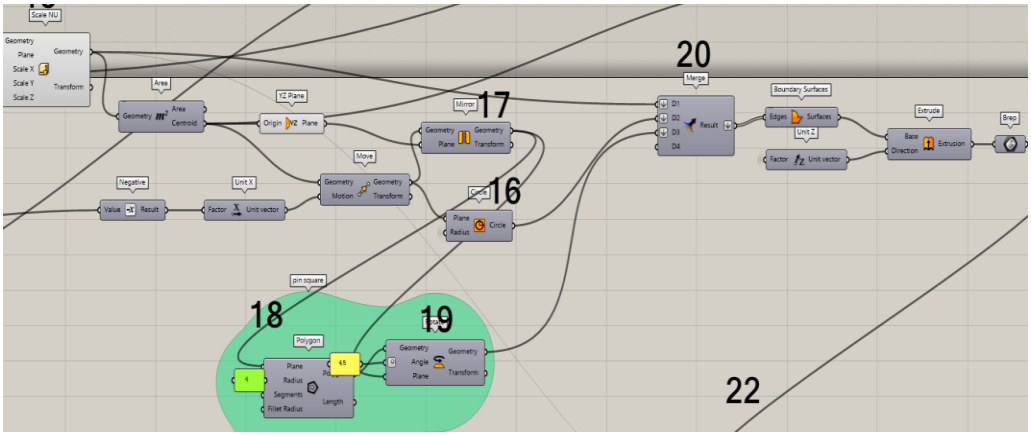

Figure 37: algorithm modelling of pins

Inputs

Name	ID	Description	Type
Plane	P	Polygon base plane	Plane
Radius	R	Radius of polygon (distance from center to tip).	Number
Segments	S	Number of segments	Integer
Fillet Radius	Rf	Polygon corner fillet radius	Number

Outputs

Name	ID	Description	Type
Polygon	P	Polygon	Curve
Length	L	Length of polygon curve	Number

Table 2: Feature of polygon component

5-In this step merge all the curve and extrude them (Figure 38). It is important to flatten all the data for getting better result by right click on the input and output data with selecting flatten.

Merge ---> Component index --->Grasshopper Sets --->tree---> Merge

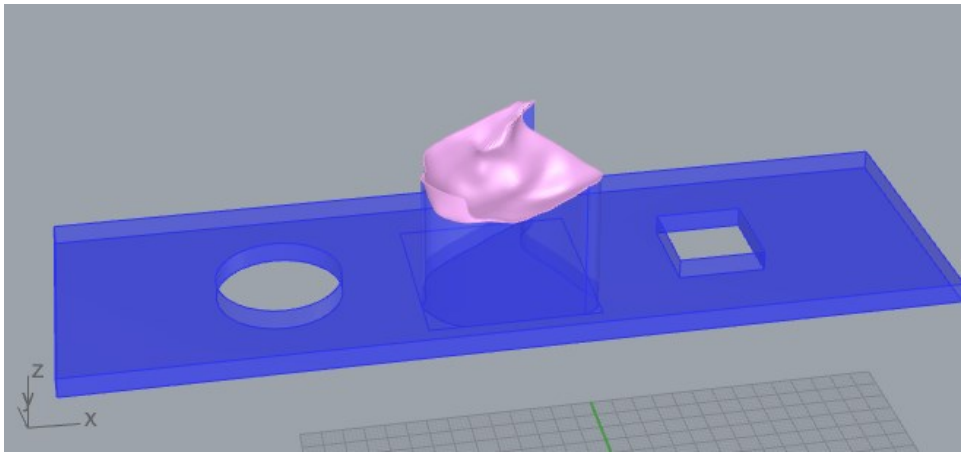

Figure 38: Adjustable surface of base plate (Die)

6- Fillet the base plate.in this part using Boolean logic for defining to the algorithm just consider the outer edge of base plate for fileting in which it is possible to adjust fillet radius (Figure 39). Fillet some edges of a brep with ***fillet*** *component has 5 input as follow:*

Shape (Brep) Shape to fillet, Blend (Integer), Metric (Integer) ,Edges (Integer) and Radii (Number) Fillet radii/measures per edge as result produce Filleted Brep .For filleting the edge of base plate we use ***dispatch component*** *in order does not consider the edge inside the base plate and just fillet the edge outside of plate in direction of Z.*

Dispatch component produce a list into two target lists. List dispatching is very similar to the [Cull Pattern] component, with the exception that both lists are provided as outputs. ***List A*** *(Generic Data) Dispatch target for True values List* ***B*** *(Generic Data) Dispatch target for False values.*

Point in Curve *component use for Test a point for closed curve containment. with this component defining just consider the points outside of the curve (Figure 40) (Table 3).*

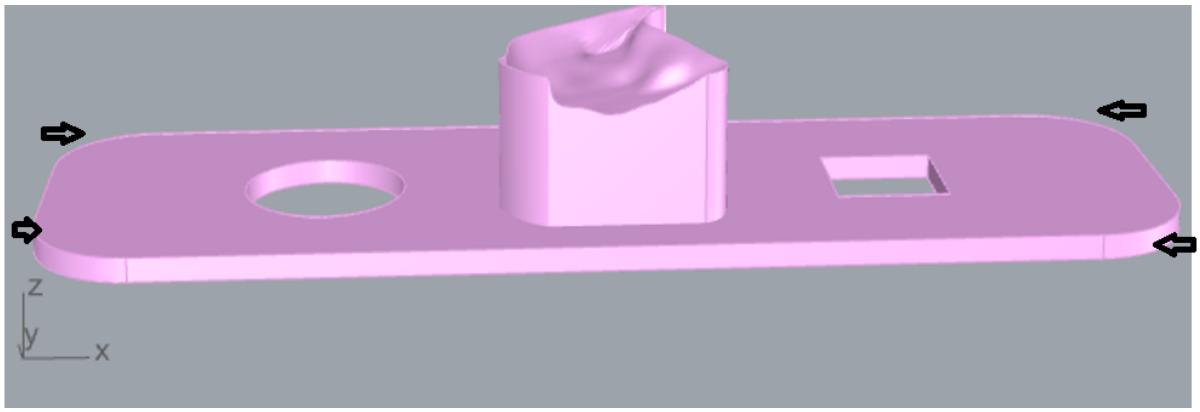

Figure 39: Fillet the edges

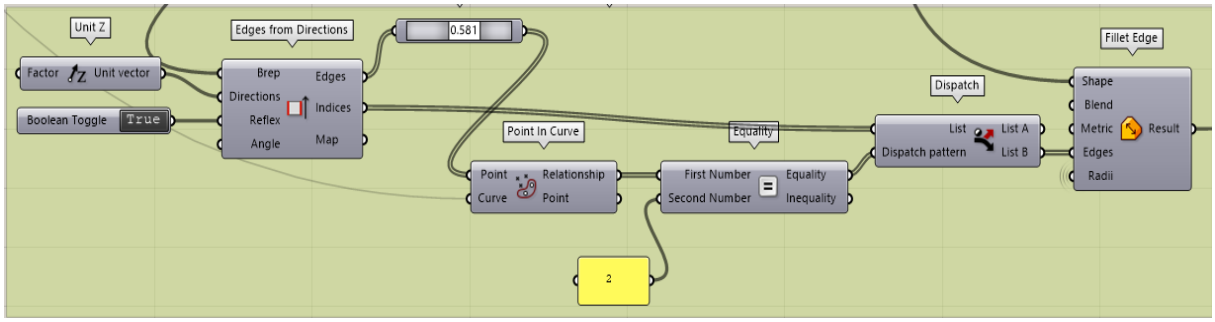

Figure 40: algorithm modelling of fillet

Point in Curves

Component Index | Grasshopper Curve | Analysis | InCurves

Test a point for multiple closed curve containment.

Inputs

Name	ID	Description	Type
Point	P	Point for inclusion test	Point
Curves	C	Boundary regions (closed curves only)	Curve

Outputs

Name	ID	Description	Type
Relationship	R	Point/Region relationship (0 = outside, 1 = coincident, 2 = inside)	Integer
Index	I	Index of first region that contains the point	Integer
Point	P'	Point projected on region plane.	Point

Table 3: Feature of point in curve component

7- So far, the base plate is completed exactly to shape of implant for the next step the floor of the base plate is move upward then extrude(Give thickness) it and make a surface for this plate (Figure 41).For this purpose deconstruct the centre of 'Scale NU plate' and perimeter of upper 'projection' of implant and calculate the height of this distance with ***subtraction*** *component. After that extrude the curves and with* ***cap holes*** *component Cap all planar holes in a Brep (Figure 42).*

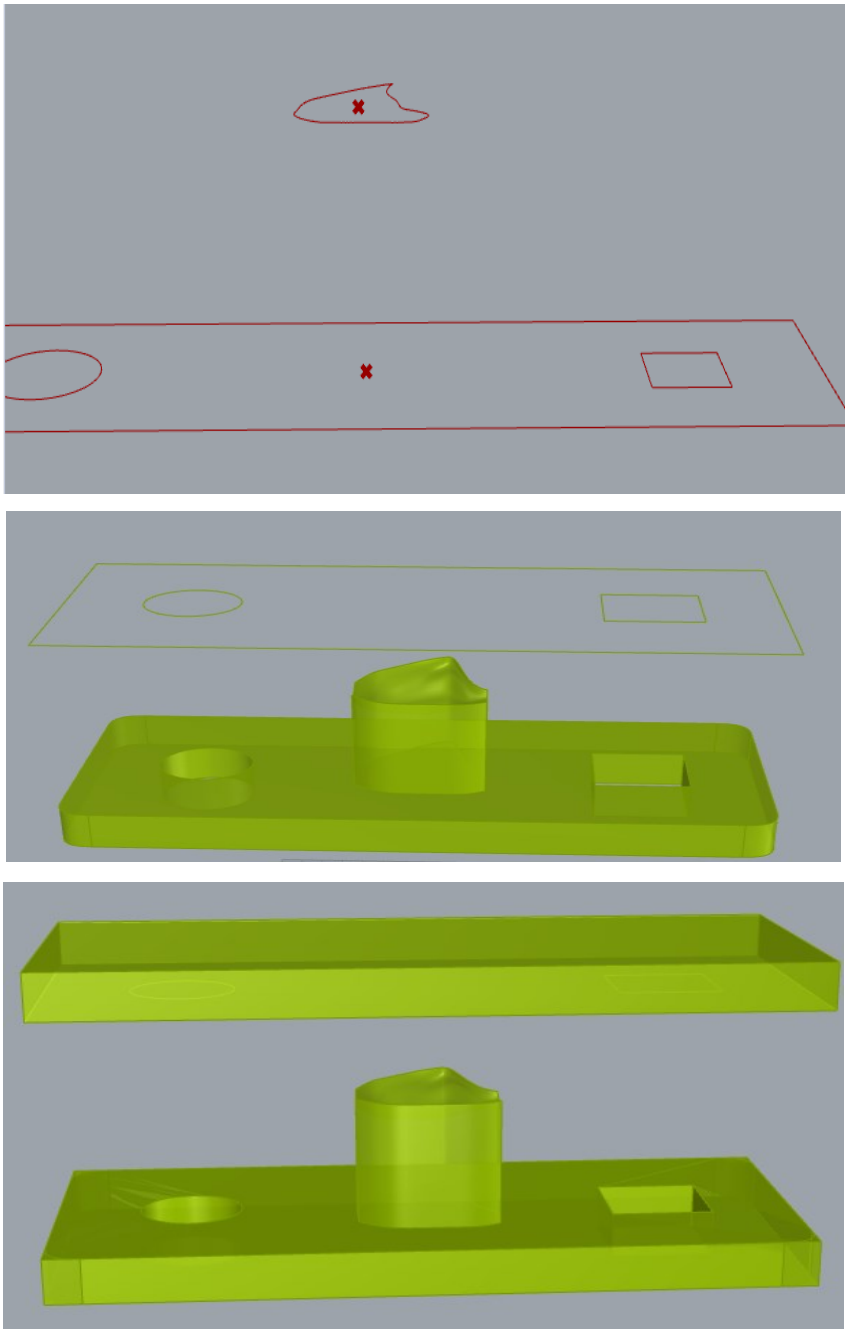

Figure 41: transferring base plate to upper side

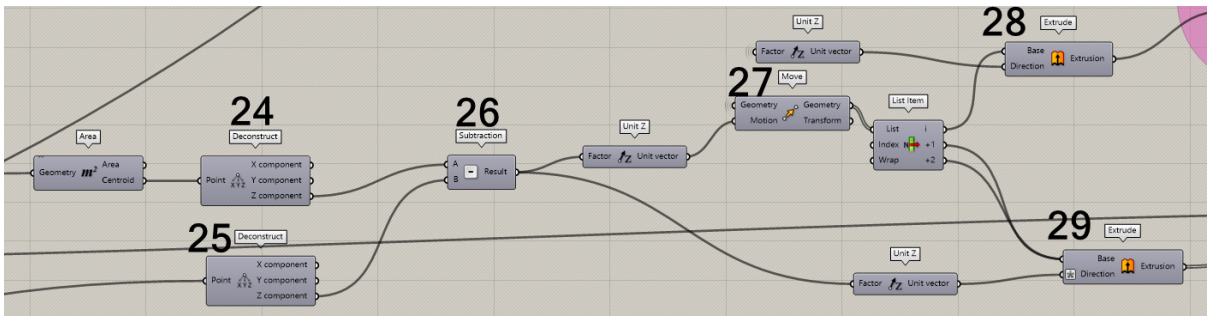

Figure 42: Algorithm modelling for designing punch

8-Then extrude the cylinder for making the pin part (Figure 43) and the shape of pins is also adjustable (for example it is possible to change the number of edges from 4 to 6).

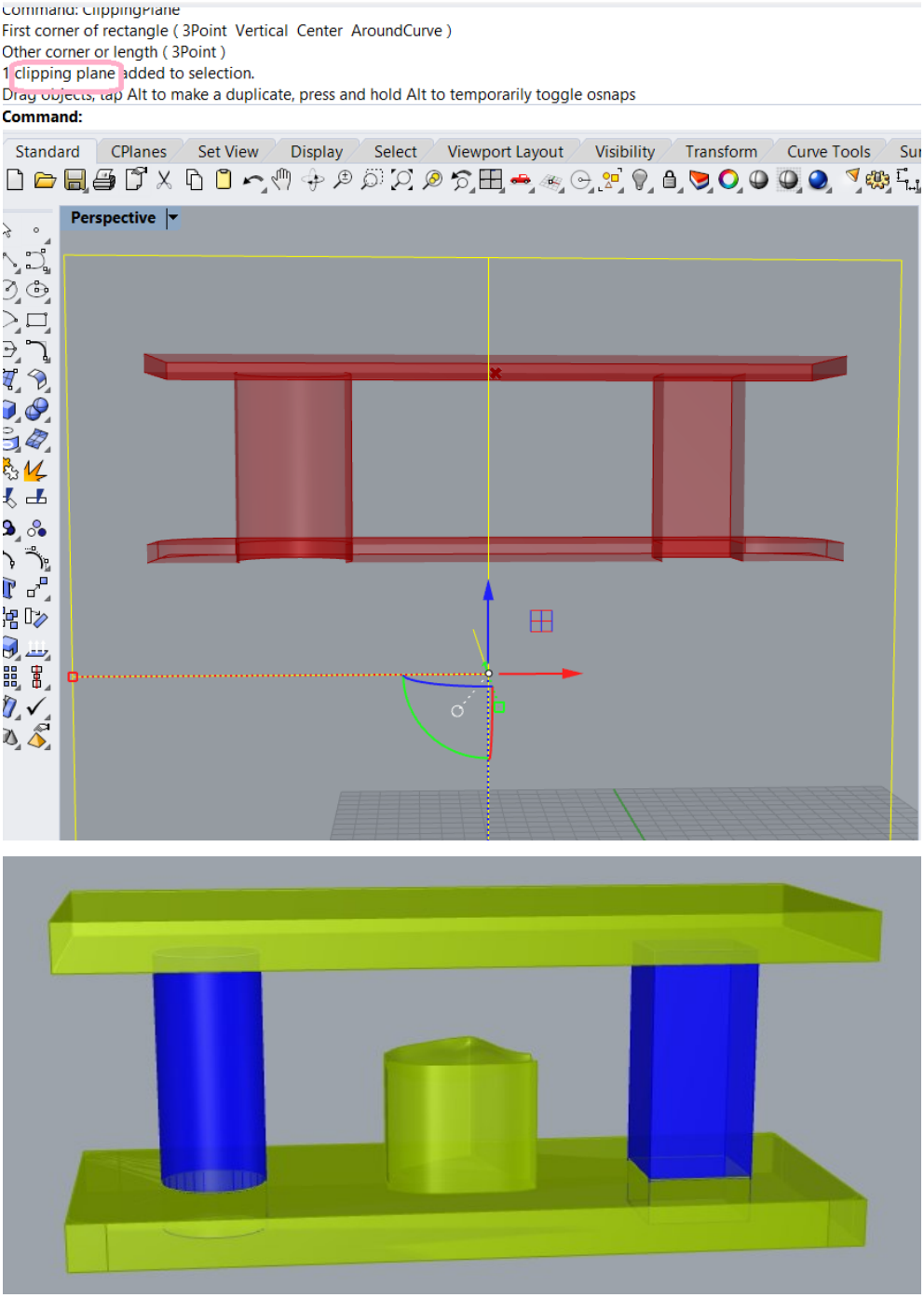

Figure 43: modelling pin part with clipping plane command see object sections

9-Fillet the edge of base plate (Die) and punch as the same value (Figure 44) which is adjustable with fillet radius slider (Figure 45). Then with ***solid union*** *component consider all the extrusion (2 pins and plate) as one solid object to be a close Brep.*

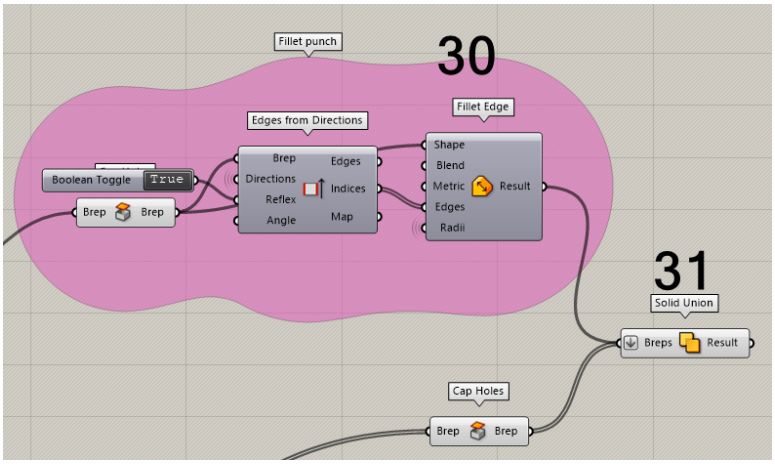

Figure 44: modelling algorithm for filleting punch

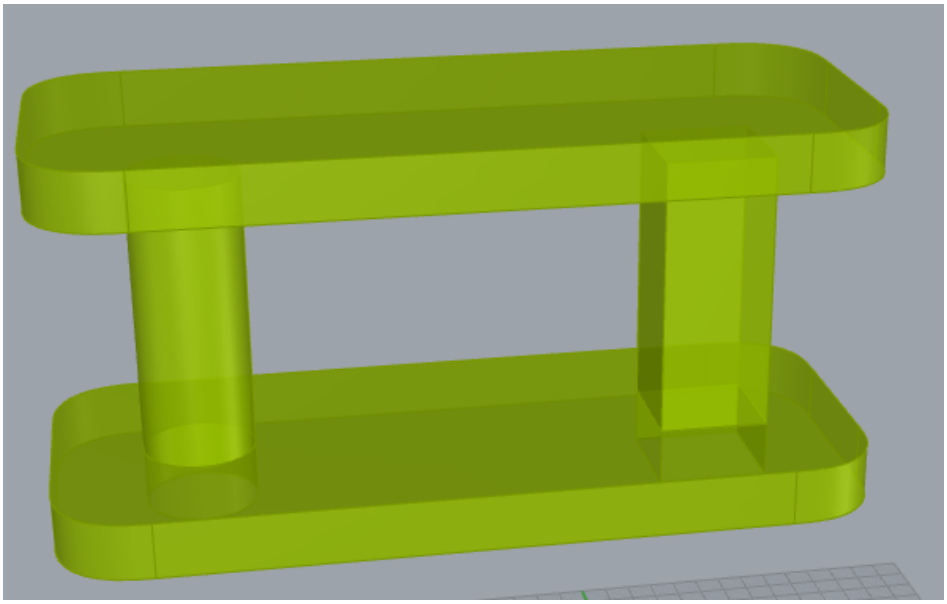

Figure 45: Punch and die fillet control by fillet slider

10-Groupe the punch and pins as one solid object to be able to move it in the direction of Z (Figure 46) that is control with the slider motion.

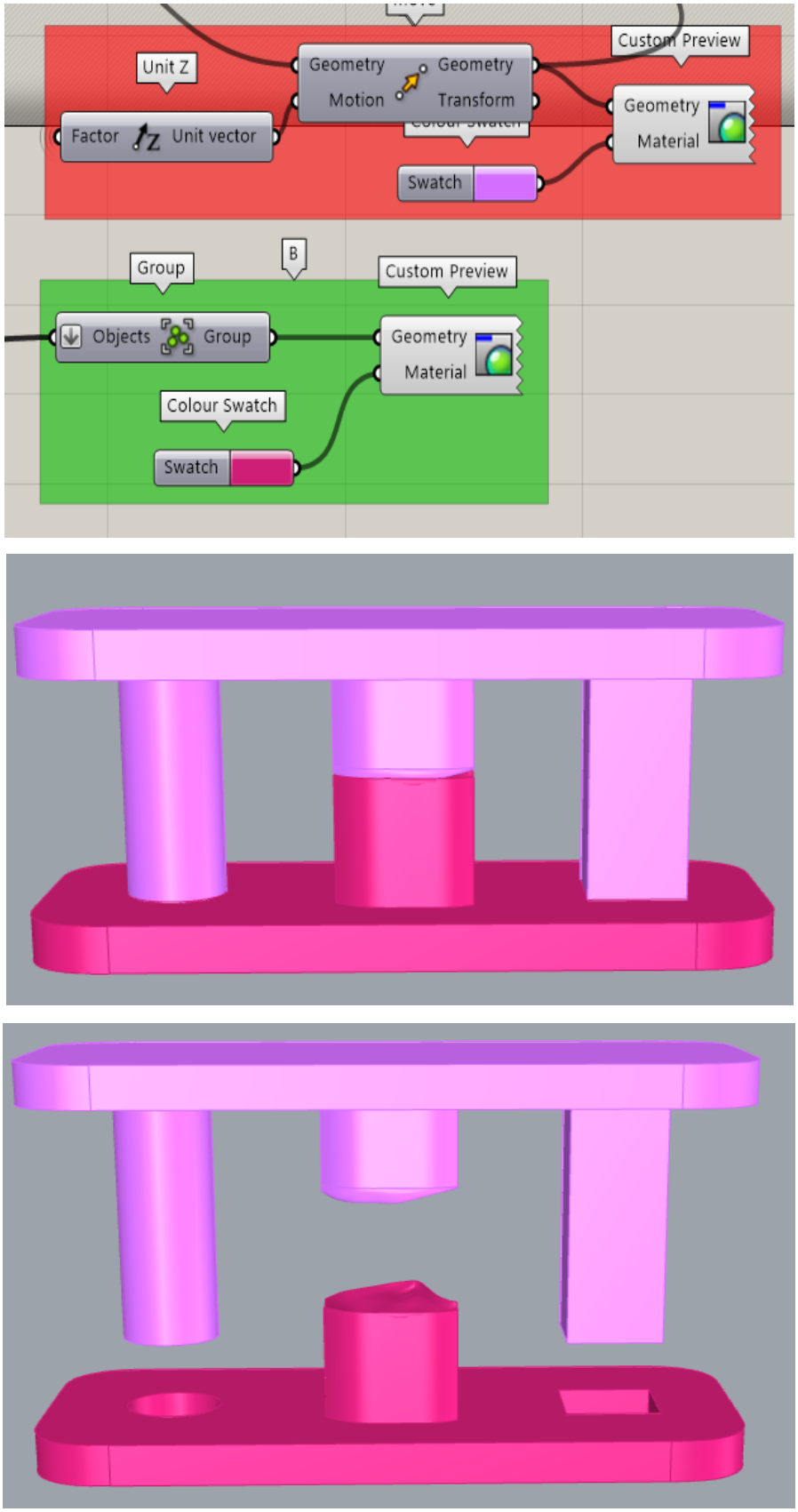

Figure 46: Group 1(Punch +implant) and Group 2(Die and active part) of the mould. Group 1 has the capability of motion

*11-For the final step give it Unit of measurement with components of '**Aligned dimension**' and '**Line dimension**' (Figure 47). This component gives the start point and the end point and calculate the distance. With component of '**Bounding box**' consider the Group 1 (Figure 48).*

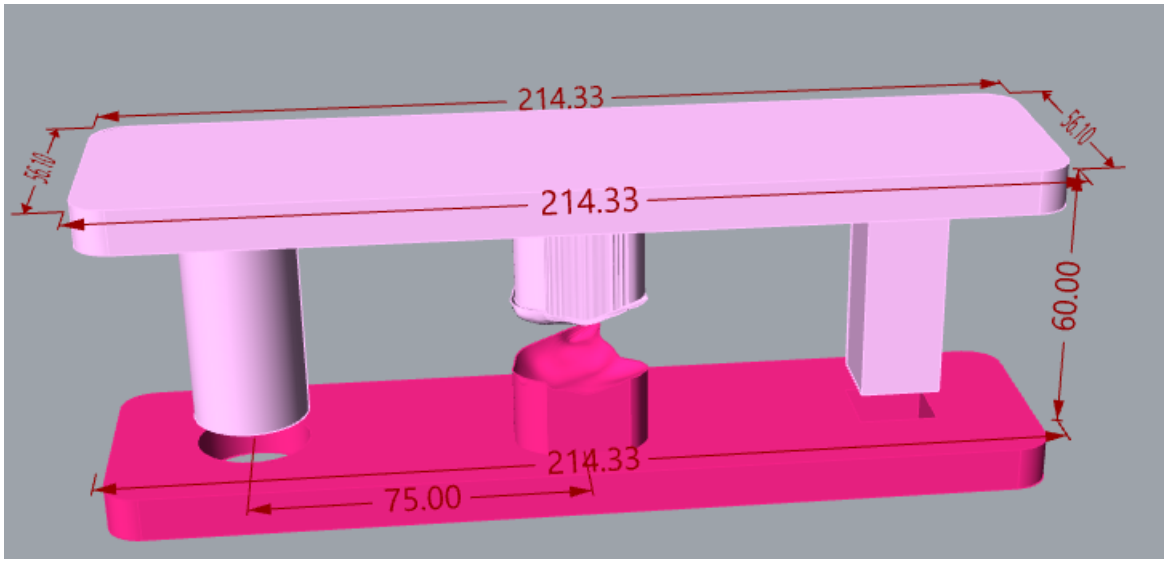

Figure 47: dimension of mould. Mould design made up of a die (pink) and a punch (purple) involved in a pressure mechanism to deform the implant material to the desired shape.

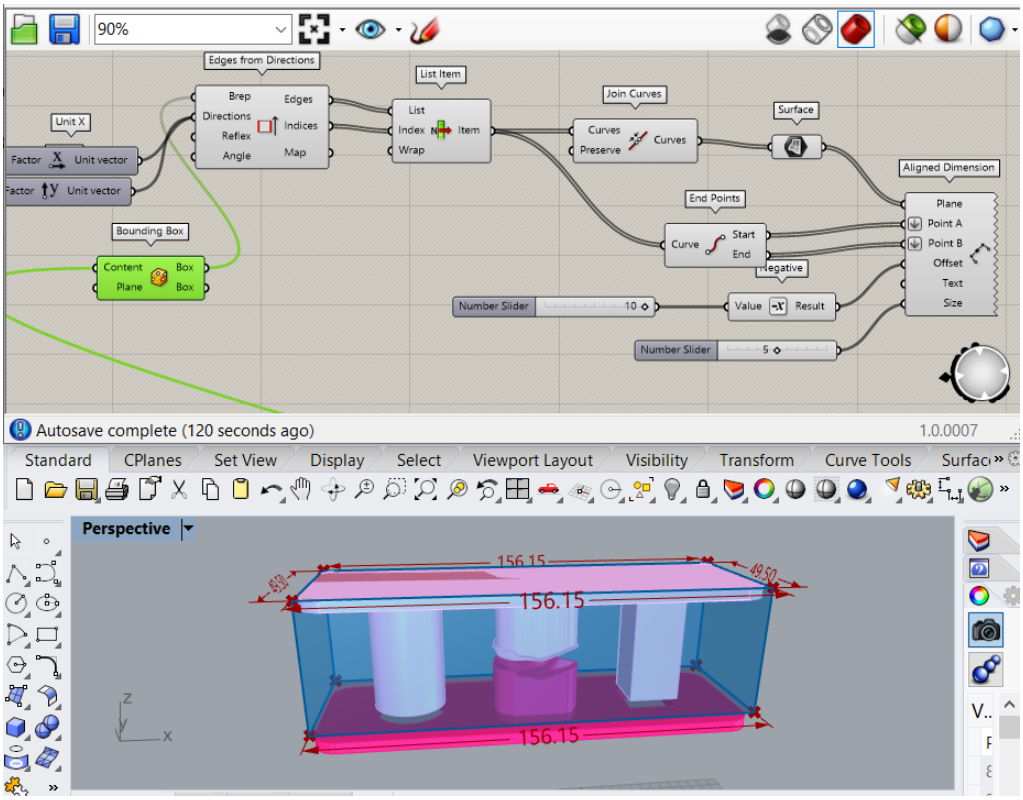

Figure 48: bounding box encompass Group 1

*For dimension of height use **'line dimension'** component by considering bonding box calculate the distance between two line (Figure).*

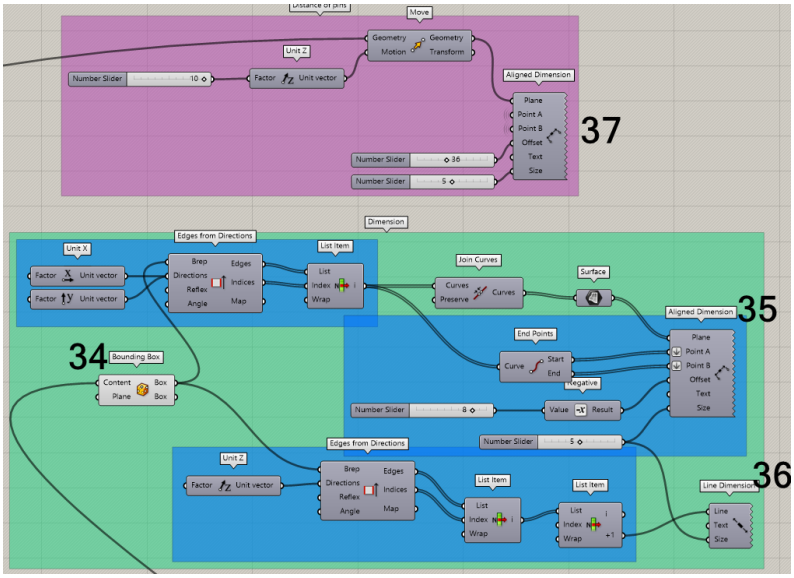

Figure 49: modelling algorithm for dimension of mould

And the Last measurement is related to the pins which are symmetric related to centre in which connect the centre of implant and centre of circle and calculate the distance between these two points. At the end save .stl file for 3D Printing production stage.

In order to work with (select, edit, transform, etc.) geometry in Rhino that was created in Grasshopper, you must "bake" it. Baking instantiates new geometry into the Rhino document based on the current state of the Grasshopper graph. It will no longer be responsive to the changes in your definition (Figure 50).

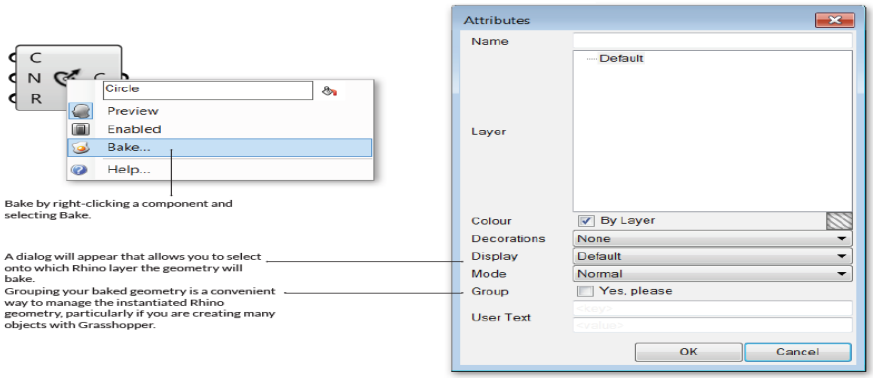

Figure 50: BAKING GEOMETRY

Baking Group 1 and Group 2 and the at the rhinoceros's software from file, save as export .stl file for rapid prototyping and with quality of 0.001 mm save the related file.

Briefly there is capability to change and control different parameters of the mould such as (Figure 51)

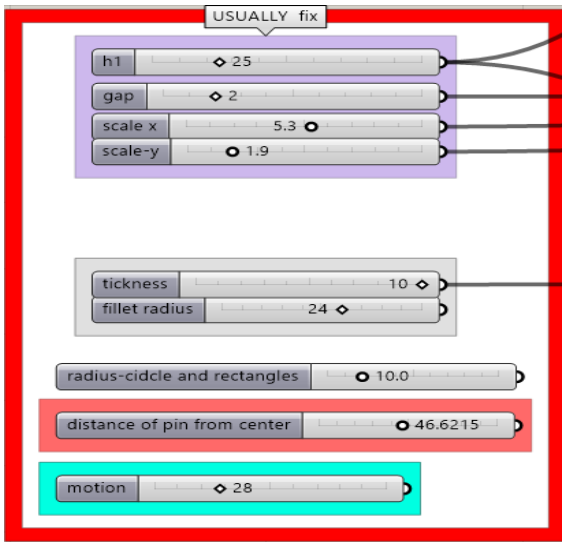

Figure 51: controllable variables of mould

4. RESULTS

This study proposed a methodological approach for the design of an implant for orbital floor fracture taking the advantage of rapid prototyping technology. A CT dataset of healthy skulls at least in the region of interest was collected and the volume of healthy eye is acquired and then mirrored it at the defect site under study and with segmentation of it and defining a surface which completely fix to floor of orbit obtaining the desired implant. for the second step by modelling the algorithm for mould that encompass the implant try to save time and improve the accuracy of the result as up to now it based on a manual procedure.

Software tools and plugins such as Grasshopper, Mimics, Rhinoceros can be useful in this regard as they allow for an easier automatic extraction of desired output.

The highly irregular anatomy of the pathological skull prevented the location of implants in the place of interest.

selection approach was totally automated and based on parameters as a customized implant requires to accurately fit the bony lesion site to guarantee continuously at the interface with the orbit.

The virtual 3D models of Grasshopper plugin resulting such as follow figures:

The first result involved a solid, compact implant as represented in (Figure 52).

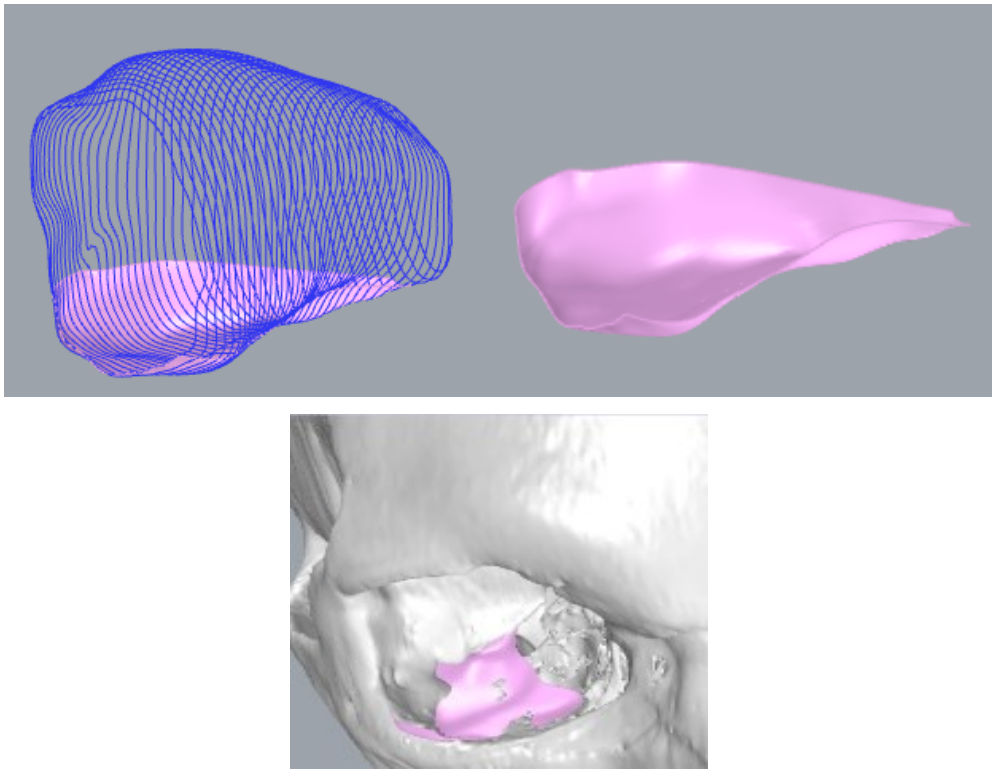

Figure 52: the modelled implant in GH

And second proposal of customized implant is designing mould that completely encompass the implant(Figure 53) .The die and the punch guides were offset by 1 mm to avoid friction in the movement (however it is possible to change the value with slider of offset)

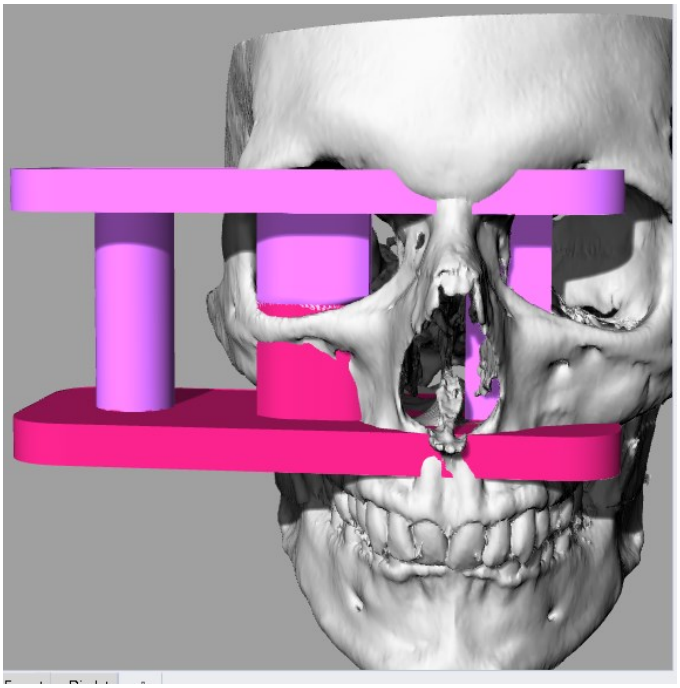

Figure 53: Implant, mould, and skull briefly in GH

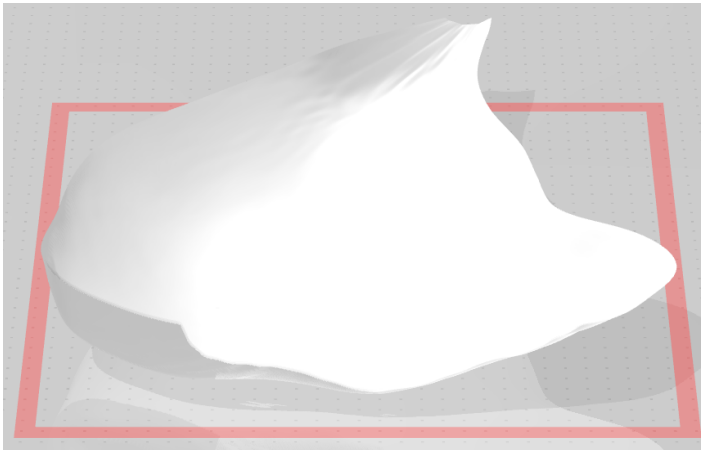

Figure 54: implant. stl format for 3D printing

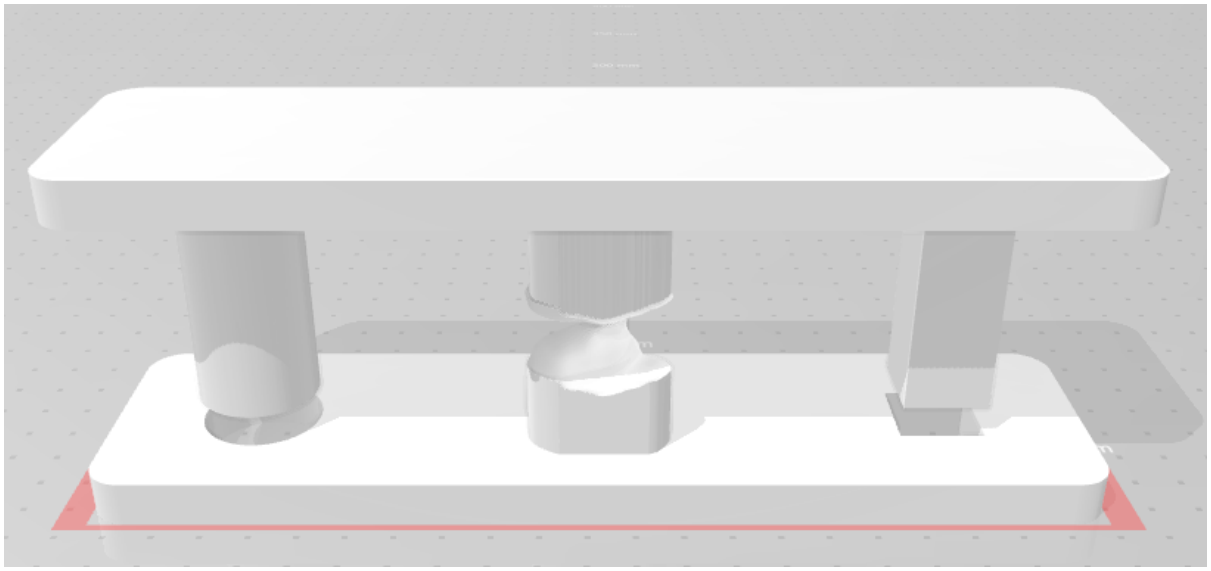

Figure 55: mould. stl format for 3D printing

5. DISCUSSION

The central question of this project asks how we can customize our designing implant during less time and decrees the time for producing implant as much as possible with high precision and secondly which manufacturing technique has better result with low cost for designing. For example, SLM technique is very expensive but Orbital fractures can be reconstructed with higher degree of accuracy with selective laser melted.

This project is methodologically focus on the designing custom made implants with 3D printing technique. Accurate restoration of the normal anatomy, symmetry, proper facial projection, and facial width are the key points in eye orbital reconstruction. Although stock-made implants are commercially available in different sizes, these implants are of limited value for repairing acquired and unusual bony defects. In contrast, custom-made patient-specific implants that are produced using computer-aided design and manufacturing (CAD/CAM) overcome these drawbacks

Although it is possible to manually shape a titanium mesh to achieve a very good approximation of the ideal reconstruction based on a 3D printed model, designing, and manufacturing the implants based on virtual models produce exceedingly accurate implants.

There are several notable advantages of this implant over a pre-bent mesh. The implants are not malleable, thus avoiding human error during the shaping stage and unwanted bending of the implants during placement. This reduces duration of surgery due to preoperative planning of correct geometrical and anatomical details [65]. The purpose of this study is to introduce a protocol for customized orbital cavity implant.

For future, the work is still developing as it is good idea to work on writing and providing plugin which help to provide, and model appropriate implant based on CT images. In addition, creating a new approach for parametric modelling to provide the volume and 3-dimensional shape of healthy orbit of eye. In addition, find an approach that could be able cut the contour with Oblique plate not just horizontally in order to have different implant dimension on the lateral and on the medial side of the orbital cavity.

The thickness of the implant is another issue to take into account. It is worth to say that the design of a custom-made implant requires a strong collaboration with the surgeon who can give advises about the shape of the implant and even the fabrication material. In this work the choice of method for supporting the orbital floor has difference with other methods for designing the implant. In other words, the mission of this literature was to Study and definition of innovative methods for designing custom-made implants for orbital cavity restoration based on Additive manufacturing Technologies. The work will consist in analysing the literature review about maxillofacial trauma surgery, then defining and testing an innovative method based on 3D printed moulds.

6. CONCLUSION

The overall goal of the work was to design and define Grasshopper algorithm to automatically designed a custom-made mould for orbital fracture. The literature describes the higher degrees of accuracy in the treatment of orbital deformities. Reconstruction of orbital walls defects is a very delicate surgery and difficult to perform and complications are mainly due to difficulties in restoring anatomy and volume. The designed implant supplies an anatomically correct fit to the orbital wall. Creating implants before surgery improves accuracy, may reduce

operation time, and decrease patient morbidity, hence improving quality of surgery [65]. This made medical 3D modelling easier because modelling software works much faster. The work is still developing thus post-implantation outcomes are not available. In other words, orbital fracture due to various situation such as accidents, fight, assaults etc require accurate and time expensive procedures for aesthetic reconstruction. Custom implants for the reconstruction of facial defects have gained importance since the advances in imaging techniques and CAD-CAM systems allowing for a precise adaptation to the region of implantation, reduced surgical times and better aesthetic outcomes. The aim of this thesis was to develop a method for designing a customized prosthesis for orbit of eye for the pathological condition. The use of alloplastic implants with specific digital design has been stated to be an effective technique on the treatment of maxillofacial defects, reducing the need for manipulation in the intraoperative period and decreasing surgery time. Polyether-ether-ketone (PEEK) is a potential candidate because its biocompatibility, stiffness and durability however the expensive costs of fabrication played a crucial role in the material selection. In fact, the second proposal of this work rely on the design of a mould to shape a different, less expensive material. Medpor is a high-density porous polyethylene containing a titanium mesh to combine strength and flexibility. It is less expensive than Peek and is widely accepted in craniofacial reconstruction. In this regard, a mould has been designed to prefabricate the customized implant.

All these proposals have been 3D printed using a polymer powder-based device for better visualization of the result and surgery simulation. Rapid Prototyping and computer modelling improved the surgical planning and the manufacture of the patient-specific implant testing its fit before the actual surgery. The creation of the mould consented the realization of a prefabricated custom implant limiting the surgical operation to the placement and fixation of the implant.

In this protocol we present an updated protocol for modelling the automatically customised algorithm for implant and mould. Last but not least, Grasshopper plugin has the capability to use more in the field of medicine for acquiring more accurate implant and prothesis for different parts of body. orbital reconstruction with use of CAD-CAM by surgeons performed within a 3D printing lab can shorten presurgical planning, facilitate intraoperative manoeuvres, and increase accuracy of reconstruction.

Index A.0

This index provides additional information on all the components used in this primer, as well as other components you might find useful.

Parameters

GEOMETRY

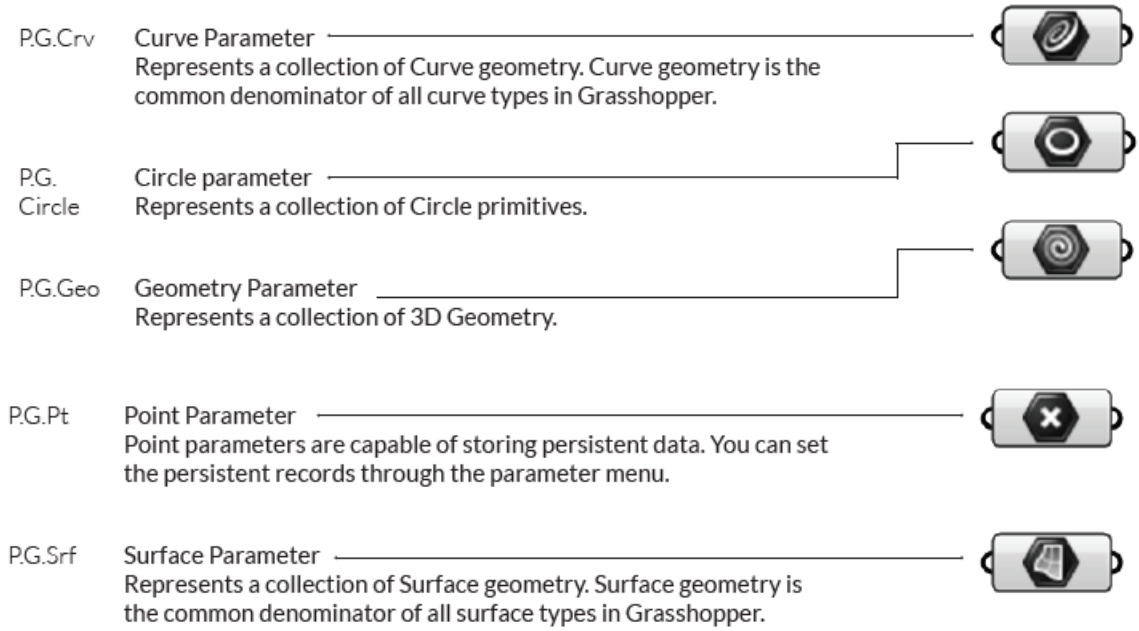

Index A.1

Components

Sets

LIST

S.L.Item **List Item**
Retrieve a specific item from a list.

S.L.Sort **Sort List**
Sort a list of numeric keys. In order for something to be sorted, it must first be comparable. Most types of data are not comparable, Numbers and Strings being basically the sole exceptions. If you want to sort other types of data, such as curves, you'll need to create a list of keys first.

POINT

V.P.Pt **Construct Point**
Construct a point from {xyz} coordinates.

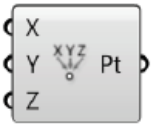

V.P.
pDecon **Deconstruct**
Deconstruct a point into its component parts.

PRIMITIVE

S.P.BBox **Bounding Box**
Solve oriented geometry bounding boxes.

Curve

Rebuild Curve

Rebuild a curve with a specific number of control-points

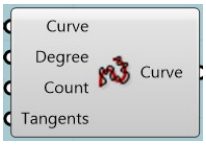

Flip Curve

Flip a curve using an optional guide curve. If more than 50% of the base curve orientation is anti-parallel to the guide curve, the base curve is flipped, and the 'flip action' is set to True. If no guide is provided, the curve is always flipped.

Bounding Rectangle

Create a plane-oriented union bounding rectangle or separate bounding rectangles for geometry.

Point in Curve

Test a point for closed curve containment.
Relationship (Integer) Point/Region relationship (0 = outside, 1 = coincident, 2 =inside)

Surface

ANALYSIS

S.A. DeBrep — Deconstruct Brep — Deconstruct a brep into its constituent parts.

Unsplit Loft Surface

Create an untrimmed lofted surface through a set of section curves or surfaces which does not split into a polysurface (Brep) at kinks.

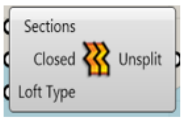

Brep Join

Join several Breps together

Edges from Directions

Select brep edges based on edge direction

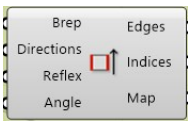

Cap Holes

Cap all planar holes in a Brep.

FREEFORM

S.F. Boundary — **Boundary Surfaces**
Create planar surfaces from a collection of boundary edge curves.

S.F.Extr — **Extrude**
Extrude curves and surfaces along a vector.

S.F.ExtrPt — **Extrude Point**
Extrude curves and surfaces to a point.

S.F.Loft — **Loft**
Create a lofted surface through a set of section curves.

S.F.RevSrf — **Revolution**
Create a surface of revolution.

S.F.Swp2 — **Sweep2**
Create a sweep surface with two rail curves.

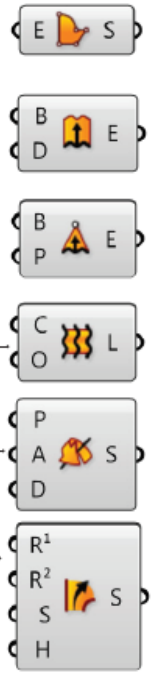

Maths

DOMAIN

M.D.Dom — **Construct Domain**
Create a numeric domain from two numeric extremes.

M.D. Dom²Num — **Construct Domain²**
Create a two-dimensinal domain from four numbers.

M.D. DeDomain — **Deconstruct Domain**
Deconstruct a numeric domain into its component parts.

M.D. DeDom² Num — **Deconstruct Domain²**
Deconstruct a two-dimensional domain into four numbers.

M.D. Divide — **Divide Domain²**
Divides a two-dimensional domain into equal segments.

M.D.Inc — **Includes**
Test a numeric value to see if it is included in the domain.

M.D. ReMap — **Remap Numbers**
Remap numbers into a new numeric domain.

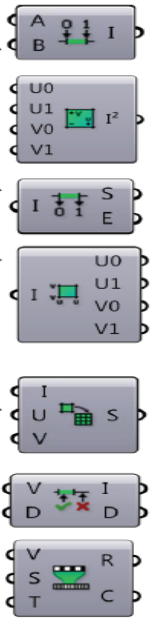

M.O.
Equals

Equality
Test for (in)equality of two numbers.

PREVIEW

D.P.
Preview

Custom Preview
Allows for customized geometry previews.

Intersect

Brep with trim

Trim a curve with a Brep.

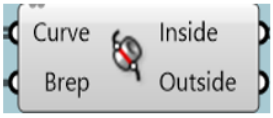

Solid Union

Perform a solid union on a set of Breps.

Transform

Project

Project an object onto a plane

Scale NU

Scale an object with non-uniform factors

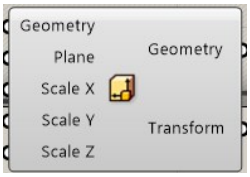

Mirror

Mirror an object

SETS

S.T.Merge

Merge
Merge a bunch of data streams.

S.L.
Dispatch

Dispatch
Dispatch the items in a list into two target lists. List dispatching is very similar to the [Cull Pattern] component, with the exception that both lists are provided as outputs.

Index A.2

There are also over a hundred plugins and add-ons that extend Grasshopper's functionality. Below are some of our favourites.in the project use bifocal and pufferfish plugin. Bifocals labelling every component that place on the canvas in real time, with the component's full name.

Bifocals

NBBJ Digital Practice is happy to release Bifocals, ending the age-old debate of Icon Display vs. Text. No matter what your preference, your tutorial watchers or students can follow along with clear, full name labels over every component you place on the canvas.

The Pufferfish is one of few animals which is capable of changing its shape.

*This plugin is a set of **318** components which focuses on Tweens, Blends, Morphs, Averages, Transformations, & Interpolations - essentially Shape Changing. Pufferfish mainly uses parameters and factors for inputs for more custom control over operations like tweens and grids as opposed to grasshopper's usual division count inputs.*

PLUG-IN COMMUNITIES

food4Rhino (WIP) is the new Plug-in Community Service by McNeel. As a user, find the newest Rhino Plug-ins, Grasshopper Add-ons, Textures and Backgrounds, add your comments, discuss about new tools, get in contact with the developers of these applications, share your scripts.
http://www.food4rhino.com/

Grasshopper add-ons page
http://www.grasshopper3d.com/page/addons-for-grasshopper

ADD-ONS WE LOVE

DIVA-for-Rhino allows users to carry out a series of environmental performance evaluations of individual buildings and urban landscapes.
http://diva4rhino.com/

Fold panels using curved folding and control panel distribution on surfaces with a range of attractor systems.
http://www.food4rhino.com/project/robofoldkingkong

Firefly offers a set of comprehensive software tools dedicated to bridging the gap between Grasshopper and the Arduino micro-controller.
http://fireflyexperiments.com

LunchBox is a plug-in for Grasshopper for exploring mathematical shapes, paneling, structures, and workflow.
http://www.food4rhino.com/project/lunchbox

GhPython is the Python interpreter component for Grasshopper that allows you to execute dynamic scripts of any type. Unlike other scripting components, GhPython allows the use of rhinoscriptsyntax to start scripting without needing to be a programmer.
http://www.food4rhino.com/project/ghpython

Meshedit is a set of components which extend Grasshopper's ability to work with meshes.
http://www.food4rhino.com/project/meshedittools

HAL is a Grasshopper plugin for industrial robots programming supporting ABB, KUKA and Universal Robots machines.
http://hal.thibaultschwartz.com/

Parametric tools to create and manipulate rectangular grids, attractors and support creative morphing of parametric patterns.
http://www.food4rhino.com/project/pt-gh

Extends Grasshopper's ability to create and reference geometry including lights, blocks, and text objects. Also enables access to information about the active Rhino document, pertaining to materials, layers, linetypes, and other settings.
http://www.food4rhino.com/project/human

Platypus allows Grasshopper authors to stream geometry to the web in real time. It works like a chatroom for parametric geometry, and allows for on-the-fly 3D model mashups in the web browser.
http://www.food4rhino.com/project/platypus

Karamba is an interactive, parametric finite element program. It lets you analyze the response of 3-dimensional beam and shell structures under arbitrary loads.
http://www.karamba3d.com/

TT Toolbox features a range of different tools that we from the Core Studio at Thornton Tomasetti use on a regular basis, and we thought some of you might appreciate these.
http://www.food4rhino.com/project/ttoolbox

Kangaroo is a Live Physics engine for interactive simulation, optimization and form-finding directly within Grasshopper.
http://www.food4rhino.com/project/kangaroo

Weaverbird is a topological modeler that contains many of the known subdivision and transformation operators, readily usable by designers. This plug-in reconstructs the shape, subdivides any mesh, even made by polylines, and helps preparing for fabrication.
http://www.giuliopiacentino.com/weaverbird/

REFERENCES

[1] Salmi, M., Tuomi, J., Paloheimo, K., Björkstrand, R., Paloheimo, M., Salo, J., Kontio, R., Mesimäki, K. and Mäkitie, A., 2012. Patient-specific reconstruction with 3D modeling and DMLS additive manufacturing. Rapid Prototyping Journal, 18(3), pp.209-214.

[2] Hammer B, Prein J. Correction of post-traumatic orbital deformities: operative techniques and review of 26 patients. J Craniomaxillofac Surg 1995;23(2):81–90

[3] JANAKARAJAH, N. and SUKUMARAN, K., 1985. ORBITAL FLOOR FRACTURES AND THEIR TREATMENT. Australian and New Zealand Journal of Ophthalmology, 13(1), pp.75-80.

[4] Pagnoni, M., Marenco, M., Ramieri, V., Terenzi, V., Bartoli, D., Amodeo, G., Mazzoli, A., & Iannetti, G. (2014). Late treatment of orbital fractures: a new analysis for surgical planning. Acta otorhinolaryngologica Italica : organo ufficiale della Societa italiana di otorinolaringologia e chirurgia cervico-facciale, 34(6), 439–445.

[5] Plotnikovs, K. and Pasters, V., 2016. The use of 3D model printing in planning distraction osteogenesys for brahymetatarsia. Foot and Ankle Surgery, 22(2), p.98.

[6] Clauser L, Galiè M, Pagliaro F, Tieghi R. Posttraumatic enophthalmos: etiology, principles of reconstruction, and correction. J Craniofac Surg 2008;19(2):351–359

[7] Hammer B, Prein J. Correction of post-traumatic orbital deformities: operative techniques and review of 26 patients. J Craniomaxillofac Surg 1995;23(2):81–90

[8] Gabrielli, M., Monnazzi, M., Passeri, L., Carvalho, W., Gabrielli, M. and Hochuli-Vieira, E., 2011. Orbital Wall Reconstruction with Titanium Mesh: Retrospective Study of 24 Patients. Craniomaxillofacial Trauma & Reconstruction, 4(3), pp.151-156.

[9] Pohlenz, P., Adler, W., Li, L., Schmelzle, R., & Klatt, J. (2012). Medial orbital wall reconstruction with flexible Ethisorb® patches. Clinical Oral Investigations, 17(2), 511-516. doi: 10.1007/s00784-012-0716-2

[10] Jank S, Emshoff R, Schuchter B, Strobl H, Brandlmaier I, Norer B (2003) Orbital floor reconstruction with flexible Ethisorb patches: a retrospective long- term follow-up study. Oral Surg Oral Med Oral Pathol Oral Radiol Endod 95:16–22

[11] C. Kai, C.Meng et al. Facial prosthetic model fabrication using rapid prototyping tools. Integrated Manufacturing Systems (2000); 11(1):42-53.

[12] M. B. Pritz, R. A. Burgett. Spheno-orbital Reconstruction after Meningioma Resection. SKULL BASE/VOLUME (2009);19(2):163-170.

[13] J.C. Carr, et al. Surface interpolation with radial basis functions for medical imaging. IEEE Trans. Med. Imag. (1997); 16:96– 107.

[14] K. Moiduddin et al. Comparing 3-Dimensional Virtual Reconstruction methods in Customized Implants. International Journal of Advanced Biotechnology and Research (2016); 7(1): 323-331.

[15] Gabrielli, M.F., Monnazzi, M.S., Passeri, L.A., Carvalho, W. R., Gabrielli, M. and Hochuli-Vieira, E. (2011), "Orbital wall reconstruction with titanium mesh: retrospective study of 24 patients", Craniomaxillofacial Trauma and Reconstruction, Vol. 4 No. 03, pp. 151-156.

[16] Tasman, W.; Jaeger, E. A., eds. (2007). "Embryology and Anatomy of the Orbit and Lacrimal System". Duane's Ophthalmology. Lippincott Williams & Wilkins. ISBN 978-0-7817-6855-9.

[17] Bertelli, E; Regoli, M (2014). "Branching of the foramen rotundum. A rare variation of the sphenoid". Italian Journal of Anatomy and Embryology. 119 (2): 148–53

[18] T.D.White, M.T.Black, P.A.Folkens. Human Osteology. Academic Press. 2011. Third edition.

[19] Teachmeanatomy.info. 2020. The Bony Orbit - Borders - Contents - Fractures - Teachmeanatomy. [online] Available at: <https://teachmeanatomy.info/head/organs/eye/bony-orbit/> [Accessed 15 October 2020].

[20] René, C., 2006. Update on orbital anatomy. Eye, 20(10), pp.1119-1129.

[21] CUNNINGHAM, J. and MARDEN, P., 1962. Blow-Out Fractures of the Orbital Floor. Archives of Ophthalmology, 68(4), pp.492-497.

[22] Monnazzi, Marcelo & Hochuli-Vieira, Eduardo & Gabrielli, Cabrini & Gabrielli, Mario & Pereira-Filho, Valfrido. (2011). Fraturas orbitais. 10. 10.5335/rfo. v10i1.1453.

[23] LIMA, Nathália & Pastori, Cláudio & MARZOLA, Clóvis & FILHO, João & Toledo, Gustavo & ZORZETTO, Daniel & Capelari, Marcos & OLIVEIRA, Marília. (2012). FRACTURE OF THE ORBITAL FLOOR TYPE BLOW-OUT LITERATURE REVIEW. Rev. Odontologia ATO. 12. 1417-1439

[24] Felding UNA. Blowout fractures - clinic, imaging and applied anatomy of the orbit. Dan Med J. 2018 Mar;65(3)

[25] Shin JW, Lim JS, Yoo G, Byeon JH. An analysis of pure blowout fractures and associated ocular symptoms. J Craniofac Surg. 2013 May;24(3):703-7.

[26] Joseph JM, Glavas IP. Orbital fractures: a review. Clin Ophthalmol. 2011 Jan 12; 5:95-100.

[27] Emodi O, Wolff A, Srouji H, Bahouth H, Noy D, Abu El Naaj I, Rachmiel A. Trend and Demographic Characteristics of Maxillofacial Fractures in Level I Trauma Center. J Craniofac Surg. 2018 Mar;29(2):471-475.

[28] Joseph JM, Glavas IP. Orbital fractures: a review. Clin Ophthalmol. 2011 Jan 12; 5:95-100.

[29] Kim HS, Jeong EC. Orbital Floor Fracture. Arch Craniofac Surg. 2016 Sep;17(3):111-118.

[30] Rana, M. and Gellrich, N., 2015. Increasing the accuracy of orbital reconstruction with selective laser melted patient-specific implants combined with intraoperative navigation. British Journal of Oral and Maxillofacial Surgery, 53(10), p.e125.

[31] Mok, D., Lessard, L., Cordoba, C., Harris, P. G., & Nikolis, A. (2004). A review of materials currently used in orbital floor reconstruction. The Canadian journal of plastic surgery = Journal canadien de chirurgie plastique, 12(3), 134–140.

[32] Pohlenz, P & Adler, W & li, Lei & Schmelzle, R & Klatt, Jan. (2012). Medial orbital wall reconstruction with flexible Ethisorb® patches. Clinical oral investigations. 17. 10.1007/s00784-012-0716-2.

[33] E. Maravelakis et al. Reverse engineering techniques for cranioplasty: a case study. Journal of Medical Engineering & Technology (2008); 32 (2): 115-121.

[34] Ventola CL. Medical Applications for 3D Printing: Current and Projected Uses. Pharmacy and Therapeutics (2014); 39(10): 704-711.

[35] R. Petzold et al. Rapid prototyping technology in medicine-basics and applications. Computerized Medical Imaging and Graphics (1999), 23: 277-284.

[36] M.Attaran. The rise of 3-D printing: the advantages of additive manufacturing over traditional manufactruring. Business Horizon (2017); 60:677-688.

[37] Aimar, Anna & Palermo, Augusto & Innocenti, Bernardo. (2019). The Role of 3D Printing in Medical Applications: A State of the Art. Journal of Healthcare Engineering. 2019. 1-10. 10.1155/2019/5340616.

[38] S. N. Kurenov, C. Ionita, D. Sammons, and T. L. Demmy,"'ree-dimensional printing to facilitate anatomic study,device development, simulation, and planning in thoracic surgery," Journal of 8oracic and Cardiovascular Surgery, vol. 149, no. 4, pp. 973–979, 2015.

[39] M. Vukievic, B. Mosadegh, J. K. Little, and S. H. Little, "Cardiac 3D printing and its future directions," JACC: Cardiovascular Imaging, vol. 10, no. 2, pp. 171–184, 2017.

[40] H. Jeon, K. Kang, S. A. Park et al., "Generation of multi-layered 3D structures of HepG2 cells using a bio-printing technique," Gut and Liver, vol. 11, no. 1, pp. 121–128, 2017.

[41] M. Randazzo, J. M. Pisapia, N. Singh, and J. P. 'awani, "3D printing in neurosurgery: a systematic review," Surgical Neurology International, vol. 7, no. 34, pp. 801–809, 2016.

[42] H. Lino, K. Igawa, Y. Kanno et al., "Maxillofacial reconstruction using custom-made artificial bones fabricated by inkjet printing technology," Journal of artificial organ, vol. 12, no. 3, pp. 200–205, 2009.

[43] W. Huang and X. Zhang, "3D printing: print the future of ophthalmology," Investigative Opthalmology & Visual Science, vol. 55, no. 8, pp. 5380-5381, 2014.

[44] T. D. Crafts, S. E. Ellsperman, T. J. Wannemuehler, T. D. Bellicchi, T. Z. Shipchandler, and A. V. Mantravadi,

[45] F. Auricchio and S. Marconi, "3D printing: clinical applications in orthopaedics and traumatology," EFORT Open Reviews, vol. 1, no. 5, pp. 121–127, 2016.

[46] M. P. Chae, W. M. Rozen, P. G. McMenamin et al., "Emerging applications of bedside 3D printing in plastic surgery," Frontiers in Surgery, vol. 16, no. 2, p. 25, 2015.

[47] C. Williams, A. James, M. P. Chae, and D. J. Hunter-Smith, "3D printing in clinical podiatry: a pilot study and review," Journal of Foot and Ankle Research, vol. 8, no. 2, p. 41, 2015.

[48] N. Guilbert, L. Mhanna, A. Didier et al., "Integration of 3D printing and additive manufacturing in the interventional pulmonologist's toolbox," Respiratory Medicine, vol. 134, pp. 139–142, 2018.

[49] S. Su, K. Moran, and J. L. Robar, "Design and production of 3D printed bolus for electron radiation therapy," Journal of Applied Clinical Medical Physics, vol. 15, no. 4, pp. 194–211, 2014.

[50] N. N. Zein, I. A. Hanouneh, P. D. Bishop et al., "'reedimensional print of a liver for preoperative planning in living donor liver transplantation," Liver transplantation, vol. 19, no. 12, pp. 1304–1310, 2013.

[51] Y. Soliman, A. H. Feibus, and N. Baum, "3D printing and its urologic applications," Urology, vol. 17, no. 1, pp. 20–24, 2017.

[52] P. Hangge, Y. Pershad, A. A. Witting, H. Albadawi, and R. Oklu, "'ree-dimensional (3D) printing and its applications for aortic diseases," Cardiovascular Diagnosis&8erapy, vol. 8, no. 1, pp. 19–25, 2018.

[53] Winder J., Bibb R. Medical rapid prototyping technologies: state of the art and current limitations for application in oral and maxillofacial surgery. J Oral Maxillofac Surg, 63 (2005), pp. 1006-1015.

[54] S.Murphy, A.Atala. 3D bioprinting of tissues and organs. Nature Biotechnlogy (2014); 32:773-785.

*[55] **Mandolini**, M., Brunzini, A., Germani, M., Manieri, S., Mazzoli, A. and Pagnoni, M., 2019. Selective laser sintered mould for orbital cavity reconstruction. Rapid Prototyping Journal, 25(1), pp.95-103.*

[56] McNeel Forum. 2020. White Paper: Creating an Editable Rhino Surface from Laser Scan Input

[57] E. Brett. Biomimetics of Bone Implants: The Regenerative Road. BioResearch Open Access (2017); 6(1).

[58] A. R. Amini et al. Bone Tissue Engineering: Recent Advances and Challenges. Rev Biomed Eng. 2012; 40(5): 363–408.

[59] Owusu JA, Boahene K (2015) Update of patient-specific maxillofacial implant. Curr Opin Otolaryngol Head Neck Surg 23:261–264

[60] Watson J, Hatamleh M, Alwahadni A, Srinivasan D (2014) Correction of facial and mandibular asymmetry using a computer aided design/computer aided manufacturing prefabricated titanium implant. J Craniofac Surg 25:1099–1101

[61] Oh J. H. (2018). Recent advances in the reconstruction of cranio-maxillofacial defects using computer-aided design/computer-aided manufacturing. Maxillofacial plastic and reconstructive surgery, 40(1), 2.

[62] Rubin JP, Yaremchuk MJ (1997) Complications and toxicities of implantable biomaterials used in facial reconstructive and aesthetic surgery: a comprehensive review of the literature. Plast Reconstr Surg 100:1336–1353

[63] Acero J, Calderon J, Salmeron JI, Verdaguer JJ, Concejo C, Somacarrera ML (1999) The behaviour of titanium as a biomaterial: microscopy study of plates and surrounding tissues in facial osteosynthesis. J Craniomaxillofac Surg 27:117–123

[64] Shah AM, Jung H, Skirboll S (2014) Materials used in cranioplasty: a history and analysis. Neurosurg Focus 36: E19

[65] Ridwan-Pramana A, Wolff J, Raziei A, Ashton-James CE, Forouzanfar T (2015) Porous polyethylene implants in facial reconstruction: outcome and complications. J Craniomaxillofac Surg 43:1330–1334

[66] J. Acero, J. Calderon, J. I. Salmeron, J. J. Verdaguer, C. Concejo, and M. L. Somacarrera, "The behaviour of titanium as a biomaterial: Microscopy study of plates and surrounding tissues in facial osteosynthesis," J. Cranio-Maxillo-Facial Surg., 1999, doi: 10.1016/S1010-5182(99)80025-0.

[67] A. M. Shah, H. Jung, and S. Skirboll, "Materials used in cranioplasty: A history and analysis," Neurosurg. Focus, 2014, doi: 10.3171/2014.2. FOCUS13561.

[68] Gokuldoss PK, Kolla S, Eckert J (2017) Additive manufacturing processes: selective laser melting, electron beam melting and binder jetting-selection guidelines. Materials (Basel) 10: E672

[69] Sidambe AT (2014) Biocompatibility of advanced manufactured titanium implants—a review. Materials (Basel) 7:8168–8188

[70] Fina F, Goyanes A, Gaisford S, Basit AW (2017) Selective laser sintering (SLS) 3D printing of medicines. Int J Pharm 529:285–293

[71] Otawa N, Sumida T, Kitagaki H et al (2015) Custom-made titanium devices as membranes for bone augmentation in implant treatment: modelling accuracy of titanium products constructed with selective laser melting. J Craniomaxillofac Surg 43:1289–1295

[72] Bandyopadhyay A, Krishna BV, Xue W, Bose S (2009) Application of laser engineered net shaping (LENS) to manufacture porous and functionally graded structures for load bearing implants. J Mater Sci Mater Med 20(Suppl 1): S29–S34

[73] Fafenrot S, Grimmelsmann N, Wortmann M, Ehrmann A (2017) Threedimensional (3D) printing of polymer-metal hybrid materials by fused deposition modeling. Materials (Basel) 10: E1199

[74] Chien SF (1998) Supporting information navigation in generative design systems. Dissertation, .2Carnegie Melon University